water

MDPI

Article

Karenia brevis and *Pyrodinium bahamense* Utilization of Dissolved Organic Matter in Urban Stormwater Runoff and Rainfall Entering Tampa Bay, Florida

Amanda L. Muni-Morgan [1,*], Mary G. Lusk [2] and Cynthia A. Heil [3]

[1] Gulf Coast Research and Education Center, School of Natural Resources and Environment, University of Florida, Wimauma, FL 33598, USA
[2] Gulf Coast Research and Education Center, Soil, Water, and Ecosystem Sciences Department, University of Florida, Wimauma, FL 33598, USA; mary.lusk@ufl.edu
[3] Mote Marine Laboratory, Sarasota, FL 34236, USA; cheil@mote.org
* Correspondence: a.munimorgan@ufl.edu

Abstract: This study investigated how nitrogen and dissolved organic matter (DOM) from stormwater runoff and rainfall support the growth of *Karenia brevis* and *Pyrodinium bahamense*. Excitation–emission matrix spectroscopy coupled with parallel factor analysis tracked changes in the optical properties of DOM in each bioassay, revealing greater reactivity of terrestrial humic-like DOM. Significant increases in cell yield and specific growth rates were observed upon additions of runoff for both species, with significant increases in specific growth rates upon the addition of a 2 in simulated rain event for *P. bahamense* only. By hour 48, 100% of the dissolved organic nitrogen (DON) in each treatment was utilized by *P. bahamense,* and by hour 72, over 50% of the DON was utilized by *K. brevis*. The percentage of bioavailable dissolved organic carbon (DOC) was greater for *P. bahamense* compared to *K. brevis,* suggesting a greater affinity for DOC compounds by *P. bahamense*. However, the bioavailability of DOM for each species could be owed to distinct chemical characteristics of labile DOM conveyed from each site. This study demonstrates that stormwater runoff and rainfall are both sources of labile DOM and DON for *K. brevis* and *P. bahamense,* which has implications for blooms of these species in Tampa Bay waters.

Keywords: harmful algal blooms; nitrogen; stormwater; dissolved organic matter; red tide; PARAFAC; Tampa Bay

Citation: Muni-Morgan, A.L.; Lusk, M.G.; Heil, C.A. *Karenia brevis* and *Pyrodinium bahamense* Utilization of Dissolved Organic Matter in Urban Stormwater Runoff and Rainfall Entering Tampa Bay, Florida. *Water* **2024**, *16*, 1448. https://doi.org/10.3390/w16101448

Academic Editor: Bommanna Krishnappan

Received: 22 April 2024
Revised: 6 May 2024
Accepted: 15 May 2024
Published: 19 May 2024

1. Introduction

Coastal eutrophication is a leading cause of water quality decline in estuaries globally due to changes in land use (i.e., agriculture, industry, and residential), non-point source pollution, fertilizer use, and fossil fuel emissions [1]. These activities have doubled the flux of nitrogen (N) from land to sea [1], resulting in the proliferation of harmful algal blooms (HABs), including blooms of species that are toxin-producers [2]. Stormwater runoff and rainfall in urbanized watersheds can be significant sources of nutrients and labile organic matter [3,4], which can range in bioavailability to specific HAB formers [5,6]. However, little is known about the fate and biogeochemical role of dissolved organic matter (DOM) conveyed from urban catchments [7]. This is due to the complexity of DOM, as it is comprised of thousands of organic compounds, delivering nutrients such as N and phosphorus (P), as well as trace metals and anthropogenic pollutants [8]. Research suggests that DOM compounds from anthropogenic sources (i.e., urban streams) are more bioavailable than DOM from vascular plant material and soils, which are considered more recalcitrant [9]. This can be due to the diagenetic alteration in soils which lowers the bioavailability [10]. Additionally, vascular plants contain high amounts of lignin in their cell walls, which is resistant to decay [11]. Urban landscapes export DOM that is typically

less aromatic and lower in molecular weight, which can be preferentially degraded by microbes [12]. Further, contributions of labile humic and protein-like DOM rich in N have been documented in urban streams [7]. These findings highlight the influence of urban land use on DOM biochemical composition and biodegradability, which has implications for downstream water quality.

One advantageous tool for characterizing fluorescent DOM (FDOM) is excitation–emission matrix (EEM) spectroscopy, as it is a fast, non-destructive measurement technique that requires no reagents and can detect fluorophores at low concentrations [13]. The result is a 3D landscape, or matrix, of excitation vs. emission vs. fluorescence intensity. FDOM is a subset of DOM, where compounds fluoresce when exposed to UV and blue light [14]. These compounds include humic substances, proteins such as tryptophan and tyrosine, pigments, and hydrocarbons [15] which have distinctive peaks that can be discriminated using parallel factor analysis (PARAFAC). In bioassay studies, the contributions of DOM from algal cultures and source water additions result in a heterogeneous mixture of chemical compounds which can have overlapping spectra. PARAFAC is a technique that can handle this overlap by decomposing the three-way array of an EEM, revealing the composition and concentration profiles of pure spectra which are most often referred to as "components" [16]. This decomposition method can be considered a form of chromatography, where the separation and identification of analytes, or components, is performed mathematically [17]. In this study, EEM spectroscopy and PARAFAC analysis of rainfall and runoff and was used for qualitative and semi-quantitative analysis of the character and subsequent evolution of FDOM when added to *K. brevis* and *P. bahamense* cultures.

Karenia brevis, the toxic dinoflagellate responsible for Florida red tide, has reoccurring blooms along the southwestern coast of Florida. Blooms result in widespread animal mortalities and risks to human health due to inhalation of a neurotoxin called brevetoxin which is released into the atmosphere via sea spray [18]. *Karenia brevis* can utilize inorganic and organic N for growth [19]. For example, cellular NH_4^+ and DON exudates excreted by the marine cyanobacterium *Trichodesium* [5] serve as an important N source in oligotrophic waters on the West Florida Shelf where blooms of *K. brevis* initiate [20]. Other organic compounds that support *K. brevis* growth include amino acids (i.e., L-valine and L-methionine) [21] and DON released from zooplankton and decaying fish [22,23]. Fluorescence monitoring of DOM during a nearshore *K. brevis* bloom detected humic-like components, suggesting that contributions of terrestrial organic matter may support blooms [24]. Further, kinetic experiments with a natural population of *K. brevis* using ^{15}N-labeled humic compounds from *Spartina alterniflora* showed an uptake of humic N [25]. This is particularly relevant when considering the potential impact of runoff on *K. brevis* blooms due to the ubiquity of humic substances in urban environments [3,26].

The occurrence of *K. brevis* red tides in association with high rainfall inputs has long been hypothesized, as outbreaks often occur at the end of the rainy season or shortly after rain events [27,28]. The proliferation of *K. brevis* blooms has been correlated with rainfall and riverine flow along the central region of Florida's gulf coast, with short lag times when observing bloom data between 1953 and 1998 [29], suggesting rainfall and subsequent stormwater runoff as a potential mechanism for bloom maintenance by delivering limiting nutrients. A more recent time-series analysis (1998–2020) showed correlations between precipitation and elevated *K. brevis* cell concentrations [30]. Additionally, the severe 2017–2019 bloom followed Hurricane Irma [31], a category 5 storm that resulted in major flooding and stormwater runoff.

Pyrodinium bahamense is a toxic dinoflagellate that blooms in Florida waters, typically in bays and estuaries with long water residence times along both coasts, namely, Tampa Bay and the Indian River Lagoon [32]. This species produces saxitoxins which cause paralytic shellfish poisoning and saxitoxin pufferfish poisoning [33] and has resulted in more human mortalities than any other HAB species [34]. Documented blooms of *P. bahamense* in Tampa Bay date back to the 1960s [35], but only since 2000 have they become an annual occurrence [36,37]. Blooms are restricted mostly to Old Tampa Bay, the northern segment

of Tampa Bay characterized by long water residence times and muck accumulation in sediments [38]. Bloom onset is typically observed in April due to warmer temperatures, lasting through October [32]. When environmental conditions are unfavorable, *P. bahamense* can form resting cysts which form 'seed beds' in the sediment that can overwinter and excyst to form new blooms in subsequent years. Organic nutrients utilized by *P. bahamense* include mangrove-derived humic substances which are mobilized during and after rain events [39]. Additionally, cultures have exhibited a prolonged exponential growth phase when soil extracts are added to the nutrient medium [39], suggesting this species may rely on terrestrial organic matter and/or nutrients in order to reach bloom cell densities.

Dramatic elevations in *P. bahamense* biomass have been associated with intense rain events, specifically in the summers of 2001–2004 in the Indian River Lagoon, and 2002 in Tampa Bay [32]. Similar responses are observed in the eastern Pacific, where blooms off the California coast correspond with increasing rainfall, with opposite trends observed during periods of drought [40]. Additionally, the occurrence of *P. bahamense* in the southeastern Gulf of Mexico has been related to anthropized sites experiencing increased nutrient inputs from stormwater outflows [41].

These data suggest that rainfall and/or stormwater runoff may influence HABs of these species by providing subsidies of nutrients and/or bioavailable DOM, leading to prolonged bloom duration and/or an increase in overall biomass. Both *K. brevis* and *P. bahamense* can utilize nutrients in inorganic and organic forms [39,42]. Therefore, this study aims to examine the biogeochemical role of nutrients and DOM from rainfall and stormwater runoff in blooms of *K. brevis* and *P. bahamense* by answering the following research questions: 1. What DOM compounds within rainfall and stormwater runoff are labile and subsequently utilized by *K. brevis* and/or *P. bahamense* for growth? 2. Can preferential DOM compounds, including those which overlap in preference between *K. brevis* and *P. bahamense*, be identified using EEM spectroscopy? 3. Will stormwater runoff contain an additional pool of bioavailable compounds vs. rainfall DOM inputs alone for each species?

2. Materials and Methods

2.1. Site Descriptions

Sampling was performed in urban residential areas within metropolitan Pinellas County, Florida, during the wet season (June and July) of 2022 (Figure 1). All stormwater runoff sites chosen within this study met the following criteria: 1. Sites are hydrologically connected to a receiving water body that is characterized as impaired [43], 2. each site delivers runoff to an area prone to recurrent blooms of *K. brevis* and/or *P. bahamense*, and 3. land use is primarily residential.

A beachside and a mainland sampling site were chosen for the *K. brevis* bioassay due to the historical spatial extent of blooms in both areas and to compare nutrient and FDOM inputs and subsequent growth responses. The first site (named Beachside) is in the city of Treasure Island, located on the western coast of Pinellas County. This site is on a dredge and fill finger island development, and land use is urban residential (7.5 dwellings per acre). Stormwater is conveyed into a curb inlet which drains directly into Boca Ciega Bay. The second site (named Mainland) is in the city of St. Petersburg along the west coast. Land use is low-density residential (5 dwellings per acre). Stormwater drainage is via an outfall pipe that exits directly into Boca Ciega Bay.

For the *P. bahamense* bioassay, stormwater was collected from two outfalls which drain directly into Old Tampa Bay. The first site (named Safety Harbor) is in the city of Safety Harbor and land use is low-density residential. The second site (named Clearwater) is in the city of Clearwater. This site receives runoff from low- to medium-density residential areas (5–15 dwellings per acre), as well as an 111-acre golf course. Rainfall (atmospheric wet deposition) was collected in an open lot devoid of tree cover located in the city of St. Petersburg.

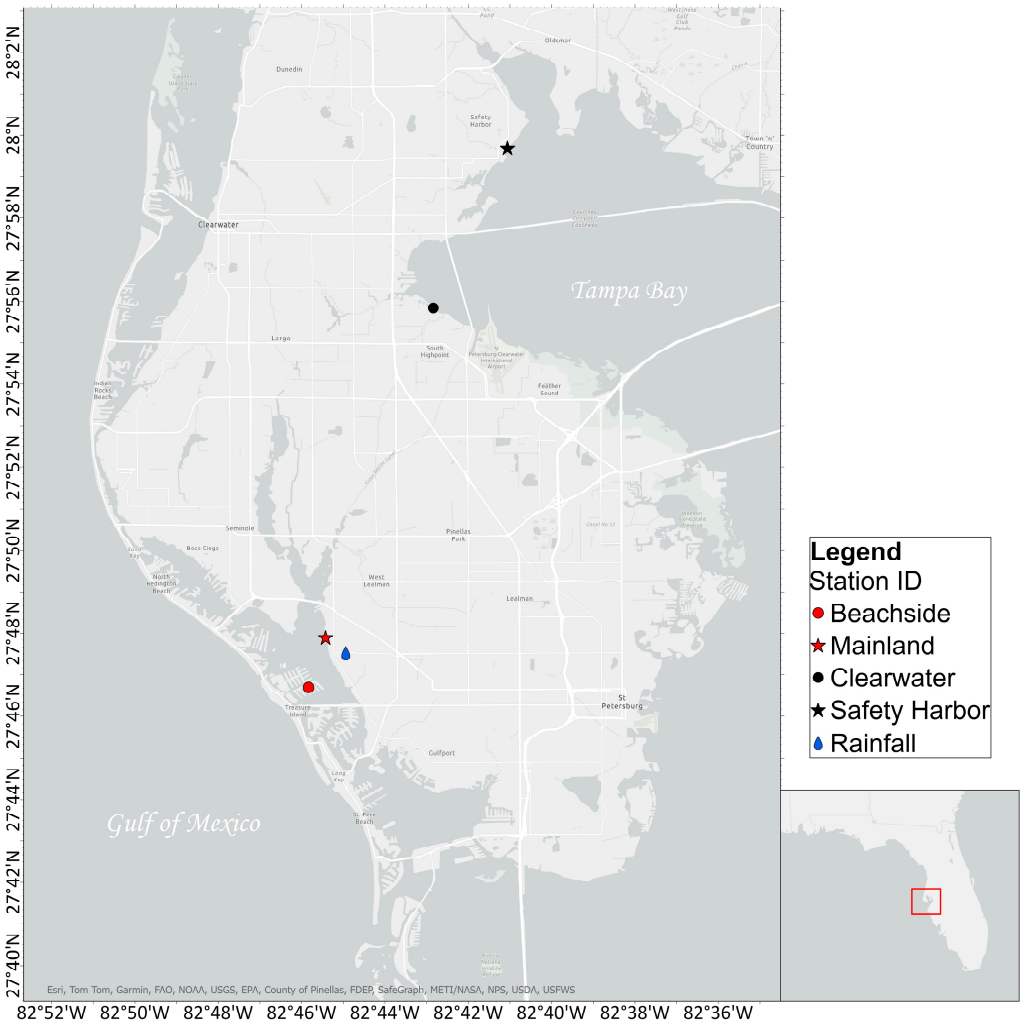

Figure 1. A map of the stormwater runoff and rainfall collection sites in Pinellas County, FL, for water used as inocula for the bioassays. The blue raindrop icon represents the rainfall collection site. Red (Beachside and Mainland) and black (Clearwater and Safety Harbor) colored icons represent sites used to collect stormwater runoff for the *K. brevis* and *P. bahamense* bioassays, respectively. The red square inset on the state of Florida to the right corresponds to the Tampa Bay region.

2.2. Sampling Regime

Storm event response sampling involved arrival at each site within 1 h of rain onset. Rainfall and stormwater were collected during a storm event in June (*P. bahamense* bioassay) and July (*K. brevis* bioassay) of 2022. Rainfall was collected using a 2.4 L acid-washed (10% HCl followed by Milli-Q rinses) sampling bucket equipped with a mesh covered funnel that was deployed prior to rainfall onset (<8 h) to minimize contributions from dry deposition particles. Sampling time and environmental conditions were recorded at each station. Grab water samples were collected at each site using a 250 mL acid-washed (10% HCl followed by Milli-Q rinses) polypropylene bottle to collect water as it enters the storm drain (i.e., Beachside) or exits an outfall (i.e., Mainland, Clearwater, and Safety Harbor), rinsing the sample bottle three times with runoff before filling, and stored in a cooler for transport to the lab. The samples were immediately filtered (sterile Pall 0.45 µm membrane) for inorganic and organic dissolved N forms, non-purgeable organic carbon (NPOC), and DOM, and immediately partitioned into acid-washed (10% HCl followed by Milli-Q rinses) polyethylene sample bottles (one sample rinse, then filled) and frozen until analysis. The filtrates to be used as the inocula during the bioassay were stored at 4 °C and filtered again (0.22 µm PES) immediately prior to dosing to enable the removal of bacteria.

2.3. Bioassay Preparation and Design

The setup for each bioassay experiment was identical for *K. brevis* and *P. bahamense* but performed separately using non-axenic laboratory cultures of *K. brevis* and *P. bahamense.* The cultures (*K. brevis* Mote Manasota Clone and *P. bahamense* FWRI Isolate 1003, Indian River Lagoon) were maintained in filtered (0.7 µm GF/F) autoclave-sterilized Instant Ocean® brand artificial seawater (salinity 35 ppt), with L1 medium nutrient additions (with the omission of Si). The cultures were maintained at 23 °C with a 12:12 L/D cycle prior to and for the duration of the bioassay. Instant Ocean® (United Pet Group, Blacksburg, VA, USA) was prepped through sequential filtration (sequential filter, 0.7 µm GF/F and 0.22 cellulose membrane) and transferred to 2.5 L acid-washed (10% HCl followed by Milli-Q rinses) glass Fernbach flasks. The cultures of *K. brevis* and *P. bahamense* (final concentrations of ~2×10^5 and ~7×10^3 cells L^{-1}, respectively) were added to each flask in triplicate and acclimated for 1 h before inoculation with stormwater/rainwater.

Inoculation concentrations for a final volume of 2 L for the low and high concentrations corresponded to a 1 cm rain event (10 mL) and a 5 cm rain event (50 mL), respectively. The concentrations were calculated based on previous bioassay studies [44,45], where a 1 cm (0.4 in) rain event corresponds to a 0.5% dilution level and a 5 cm (2 in) rain event corresponds to a 2.5% dilution in a 2 m well-mixed water column. The volume of stormwater runoff added matched the high rainfall dose (50 mL) to enable a direct comparison of response between the treatments. Control treatments received 50 mL of filtered MIQ (0.22 µm PES) water. Samples (20 mL) were collected at hours 0, 24, 72, and 120 (*K. brevis*) and hours 0, 24, 48, 96, and 144 (*P. bahamense*) and preserved (Lugol's solution) for later microscopic enumeration of cells using a Labomed TCM 400 Inverted Phase Contrast Digital HD microscope (Labo America Inc., Fremont, CA, USA). The preserved cell samples were gently inverted 10 times, pipetted into a Sedgewick rafter counting chamber (volume 1 Ml), and allowed to settle for 20 min prior to microscopic enumeration.

2.4. Nutrient Analysis

For each bioassay, water was collected at hours 0, 24, 72, and 120 (*K. brevis*) and hours 0, 48, 96, and 144 (*P. bahamense*), filtered (sterile Pall 0.45 µm membrane), and sub-sampled into acid-washed (10% HCl followed by Milli-Q rinses) high-density polyethylene bottles. The bottles were frozen (−20 °C) for later analysis of NPOC, total dissolved nitrogen (TDN), ammonium (NH_4-N), and nitrate plus nitrite (NO_x-N). A separate bottle was reserved for DOM analysis at the initial and final timepoints for each bioassay, and the bottles were then stored frozen (−20 °C) in a brown paper bag to prevent photodegradation of DOM. NPOC (hereafter referred to as dissolved organic carbon (DOC)) and TDN concentrations were measured by means of combustion catalytic oxidation using a Shimadzu TOC-L analyzer (Shimadzu U.S.A. Manufacturing, Inc., Canby, Oregon, USA). Ammonium and nitrate plus nitrite were analyzed using the salicylate method (Seal method G-102-93) and the sulphanilamide method (Seal method G-109-94), respectively, using a Seal AA3 continuous segmented flow analyzer (SEAL Analytical Limited, Mequon, WI, USA). The DON was calculated as the difference between the TDN and DIN.

2.5. DOM Optical Analysis

Spectrofluorometric analysis (EEM and absorbance spectra) of the bioassay, stormwater runoff, and rainfall DOM samples was performed using a HORIBA Scientific Aqualog® (Horiba Instruments Inc., Irvine, CA, USA) to identify the initial chemical composition of the source water and to track subsequent transformations. The samples were thawed, brought to room temperature, and analyzed in an acid-soaked (10% HCl; 24 h) 1 cm quartz cuvette, which was rinsed 20 times with Milli-Q water and once with sample water before being scanned. Prior to sample analysis, validation checks for water Raman peak signal to noise and emission calibration were performed, as well as standardization of fluorescence intensity in quinine sulfate units (QSU) using a 1 ppm standard of quinine sulfate solution scanned at an excitation wavelength of 347.5 nm. Excitation wavelengths were measured

from 239 to 800 nm (3 nm increments), and emission wavelengths were measured from 248 to 827 nm (5 nm increments) for all sample EEMs. An integration time of 4 s with a high gain setting and an integration time of 2 s with a medium gain setting were used for the bioassay and stormwater samples, respectively. Fluorescence EEM spectral correction was performed through subtraction of a sample blank of Milli-Q water to remove Raman scatter. EEMs were also corrected for IFE and 1st and 2nd order Rayleigh scattering and normalized to the Raman peak of the Milli-Q water (Aqualog Software v 3.6) to enable a direct comparison of relative fluorescence between all sample EEMs.

2.6. Fluorescence and UV Indices

Additional optical proxies were measured using the EEM and absorbance spectra to further resolve the composition and chemical nature of DOM using the staRdom package in 'Rstudio' (version 4.2.2) [46]. Specific ultraviolet (UV) absorption at 254 nm ($SUVA_{254}$) was determined for all EEMs by using the absorbance values measured at 254 nm, dividing that value by the corresponding DOC concentration, and subsequently averaging each triplicate. This proxy was utilized as it can be used to determine humic content and the degree of aromaticity of DOM [47], thus providing insight into potential reactivity. The humification index (HIX) was calculated to determine the degree of humification, or the shift in emission spectra toward longer wavelengths [48]. Humification is a microbially mediated process of transforming lower molecular weight compounds, such as those originating from plant and animal residues, to higher molecular weight, condensed compounds [49]. The calculation for HIX is performed by dividing the sum of the emission intensity in the 435–480 nm region by the sum of the total fluorescence intensities between the 300–345 and 435–480 nm regions [48]. The resultant value is between 0 and 1, with 1 indicating the highest degree of humification [48]. The biological index was calculated to determine recent autochthonous production of DOM [13]. BIX is calculated by dividing the fluorescence intensity of emissions 380/430 nm, which were measured at an excitation wavelength of 310 nm, with values > 1 indicating a predominantly autochthonous origin [13].

2.7. PARAFAC Modeling

A PARAFAC model was created in PLS_Toolbox v 9.2 (Eigenvector Research Inc., Manson, WA, USA) in MATLAB (R2023a) to determine the underlying fluorophores in all samples, utilizing the methods outlined in Stedmon and Bro [14]. Two PARAFAC models were created, the first which included the source water (stormwater and rainfall) used as inocula (SW-MOD, n = 6), and the second which included samples from each bioassay (n = 60), comparing initial and final timepoints (BIO-MOD). The creation of the two models was due to higher fluorescence in the stormwater source water, which imparted higher leverage on the combined model. Non-negativity constraints were placed on both models. EEM filtering settings included a 10 nm first order and 20 nm second order Rayleigh filter (BIO-MOD) and a 15 nm first order and 30 nm second order Rayleigh filter (SW-MOD), which were subsequently replaced with interpolated values. Emission spectra below 275.362 nm and above 698.746 nm were removed for SW-MOD to eliminate noise peaks. Emission wavelengths above 646.533 nm were removed for BIO-MOD to eliminate noise peaks and to improve model fit. Both models were validated through core consistency diagnostic measurements, split-half analysis, as well as examination of residuals, as outlined in Murphy et al. [50]. The core consistencies were 93 and 79, and the results for split-half analysis were 79.6% and 85.3% for BIO-MOD and SW-MOD, respectively. The resultant models explained 96% and 99% of the data for BIO-MOD and SW-MOD, respectively, generating a 3-component model for BIO-MOD and a 2-component model for SW-MOD.

Both models were exported to the online spectral database OpenFluor to match underlying components to the existing literature. OpenFluor enables a direct quantitative comparison of fluorescence spectra by using Tucker congruence, which measures similarity (typically ≥ 0.95) on the uploaded emission and excitation spectra simultaneously [51]. A

0.95 Tucker congruence coefficient threshold was set for excitation and emission for both models. FDOM peaks were further compared visually to the commonly described Coble peaks (Table 1) [52–54].

Table 1. Comparison of bioassay and source water PARAFAC model peaks with existing designations outlined by Coble [52,55]. Excitation and emission spectra are expressed in nm. Secondary excitation peaks are in parentheses.

Present Study	Coble Peak Assignments	Designation
C1: <250 (329)/440	A: 260/400–460	UVC humic-like
	C: 320–360/420–460	UVA humic-like
C2: <250 (296)/403	M: 290–310/370–410	UVA marine humic-like
C3: 266/290	B: 275/305	Tyrosine/protein-like
SW1: <250 (284)/413	A: 260/400–460	UVC humic-like
SW2: 260 (380)/491	D: 390/509	Soil fulvic-like

2.8. Statistical Analysis

Linear modeling and statistical testing for maximum cell concentrations and growth rates for both bioassays were performed using 'Rstudio' (v 4.2.2). Specific growth rates expressed as divisions per day were calculated by log transforming the cell count data and using time intervals that represent linear exponential growth [56]. The distribution of the data failed to meet the assumption of normality and were subsequently log-transformed prior to modeling. The *glmmTMB* package [57] was used to fit the models (negative binomial for maximum cell concentrations; gamma for growth rates) and measure the significance ($p \leq 0.05$, 95% confidence) between treatments. Overdispersion of the data was tested using the *performance* package [58]. Homogeneity and normality of the model residuals were examined and simulated using the *DHARMa* package [59] to validate model fit, and further examined using histograms and qqplots (*car* package [60]). A type II Anova test was performed using the *car* package to compare group means between treatments. The *emmeans* package [61] was used for pairwise post hoc comparisons of means for maximum cell concentrations and growth rates between sample treatments. Means and confidence intervals were back-transformed from the log scale. A confidence level of 0.95 was used, and resultant *P* values for pairwise comparisons of means were adjusted using the Tukey method.

3. Results

3.1. PARAFAC Modeling of Bioassay and Inoculum Water

The Openfluor database search of BIO-MOD generated 62, 11, and 7 matches for component 1 (C1-humic), component 2 (C2-microbial humic), and component 3 (C3-protein), respectively. Fluorescence EEMs and the corresponding excitation/emission spectra can be seen in Figure 2. C1-humic has two excitation maxima at <250 and 329 nm, and one emission maximum at 440 nm. C1-humic is defined by Coble et al. as humic-like peaks A and C, and has been observed in both terrestrial and marine DOM, with minor differences in peak positions [53,62]. Peak A fluoresces in the UV range, while peak C fluoresces in the visible range [15]. Peaks A and C are generally considered terrestrial humic substances of allochthonous origin [63,64]; however, C1-humic was observed in Control treatments for both bioassays, void of additions of terrestrial DOM. To rectify this overlap, HIX was used to distinguish humic fluorescence produced *in situ* vs. introduced via stormwater as the shift in emission spectra toward longer wavelengths [48] can be indicative of terrestrial humic substances due to increased aromaticity [65]. Conversely, marine humic-like fluorescence exhibits shorter (blue-shifted) excitation and emission maxima [53,66]. C2-microbial humic has two excitation maxima at <250 and 296 nm, and one emission maximum at 403 nm. C2-microbial humic, commonly defined as Coble peak M, is described as autochthonous marine humic-like DOM of recent biological origin [53,67]. Peak M can also be considered

a microbially derived humic substance of recent origin from terrestrial environments [68]. C3-protein has an excitation/emission maximum of 266/290 nm and is identified as a protein-like component [69], similar to Coble peak B which is defined as tyrosine-like [53].

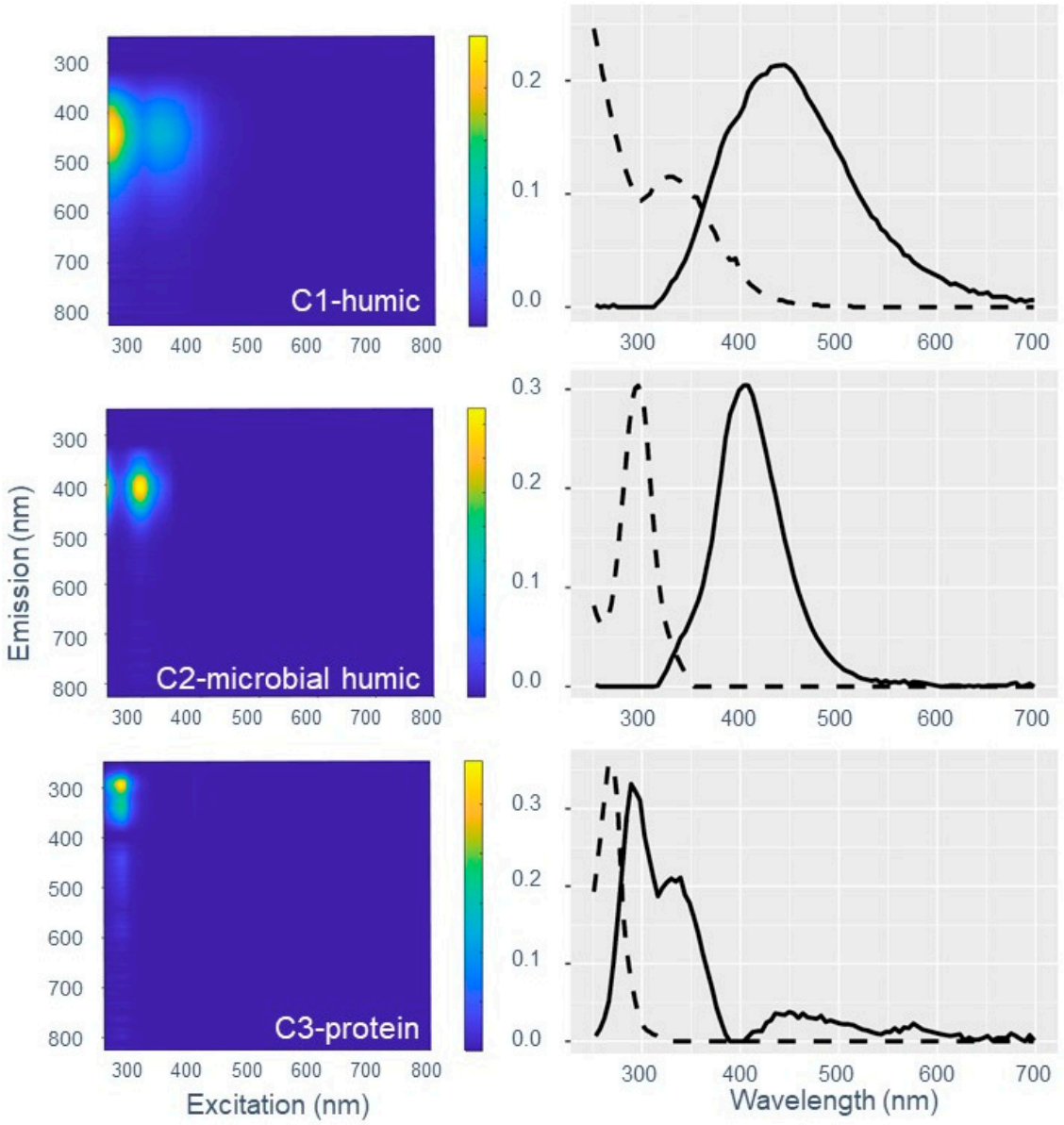

Figure 2. Fluorescence signatures of PARAFAC modeled BIO-MOD components from the *K. brevis* and *P. bahamense* bioassays. The EEM contour plots (**left panel**) for each component are displayed with emission wavelengths (nm) on the Y-axis, excitation wavelengths (nm) on the X-axis, and a colored scale bar representing fluorescence intensity in quinine sulfate units (QSU) from low (blue) to high (yellow). The corresponding excitation/emission spectra for each component are placed to the **right**. The dashed/solid lines represent excitation/emission spectra wavelengths (nm), respectively, with the Y-axis representing fluorescence intensity in QSU.

SW-MOD was fitted using the source water only (stormwater and rainwater) to minimize leverage due to increased fluorescence in the stormwater samples. Fluorescence EEMs and the corresponding excitation/emission spectra can be seen in Figure 3. SW-MOD is a two-component model, and both components exhibit combinations of Coble peaks A and C indicative of terrestrial humic substances [53], with slight shifts in their respective excitation/emission maxima. The first component (SW1-terrestrial humic) is considered

terrestrial humic-like [70] and has similar spectral characteristics of DOM found in urbanized eutrophic environments [71]. SW1-terrestrial humic has two excitation maxima at <250 and 284 nm, and one emission maximum at 413 nm. This component matches closely with Coble peak A [53]. SW1-terrestrial humic was the dominant contribution of FDOM in all source water (Figures 3–6).

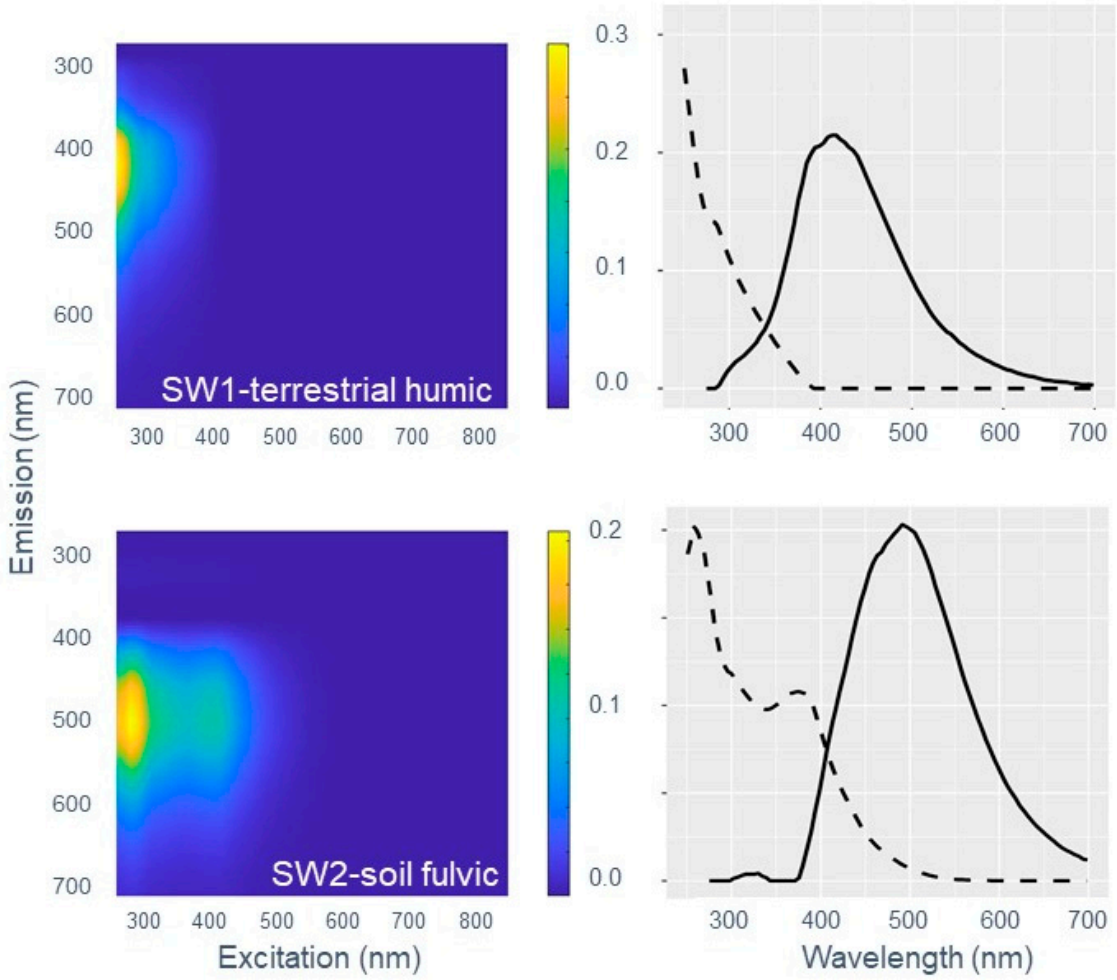

Figure 3. Fluorescence signatures of PARAFAC modeled SW-MOD components from the source water used as the inoculum for the *K. brevis* and *P. bahamense* bioassays. The EEM contour plots (**left panel**) for each component are displayed with emission wavelengths (nm) on the Y-axis, excitation wavelengths (nm) on the X-axis, and a colored scale bar representing fluorescence intensity in quinine sulfate units (QSU) from low (blue) to high (yellow). The corresponding excitation/emission spectra for each component are placed to the (**right**). The dashed/solid lines represent excitation/emission spectra wavelengths (nm), respectively, with the Y-axis representing fluorescence intensity in QSU.

The second component (SW2-soil fulvic) is another terrestrial humic-like component which closely resembles DOM from soil fulvic acids [72]. This peak is slightly red-shifted from SW1-terrestrial humic, with two excitation maxima (260 and 380 nm) and one emission maximum at 491 nm. This component closely resembles Coble peak D [53]. SW2-soil fulvic contributed very little to the overall fluorescence in rainfall source water used for each bioassay (1.6% for *P. bahamense*; 9.4% for *K. brevis*).

Due to the lack of C2-microbial humic and C3-protein in SW-MOD, it can be concluded that these components are autochthonously produced by *K. brevis* and *P. bahamense*. Both peaks M and B have been shown to be produced by marine phytoplankton [73,74] and bacteria [75].

3.2. FDOM Transformations

Changes in the relative fluorescence comparing initial and final timepoints revealed contrasting changes in FDOM for each species and FDOM component (Figures 4 and 5). For the *K. brevis* bioassay, 4%, 42%, and 25% reductions in C1-humic were observed for the Rain High, Beachside, and Mainland treatments, respectively (Table 2). The reductions in C2-microbial humic were 100%, 98%, 96%, and 35% for Control, Rain Low, Rain High, and Mainland treatments, while a slight increase in C2-microbial humic for the Beachside treatment (8%) was observed. The reductions in C3-protein were 75%, 59%, and 20% for Control, Rain Low, and Mainland treatments, but increases of 16% and 3995% for Rain High and Beachside treatments were observed, respectively.

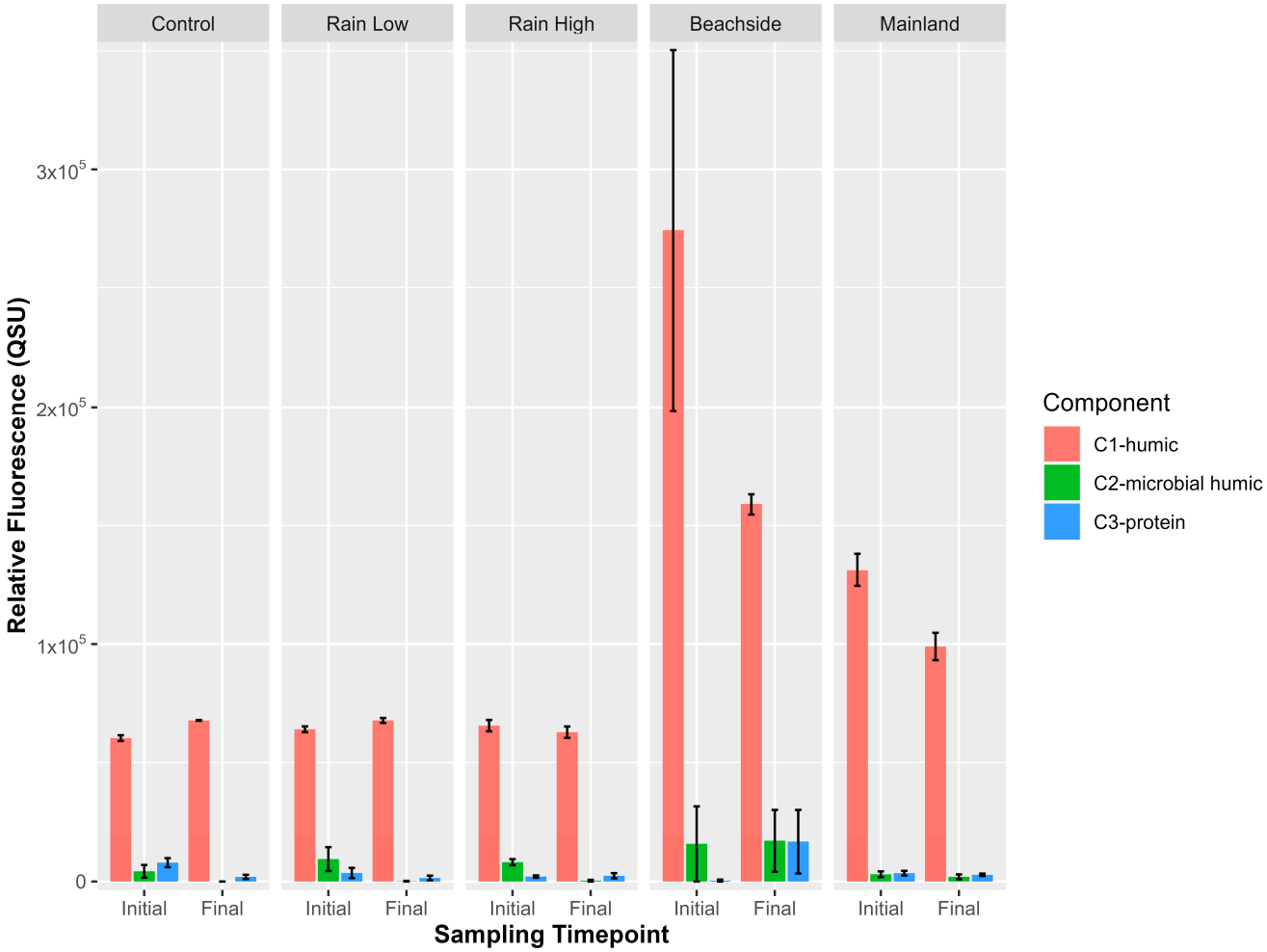

Figure 4. Changes in the relative fluorescence of FDOM components for the *K. brevis* bioassay. The colored bars represent individual components generated from the PARAFAC model, with comparisons between initial and final sampling timepoints for each treatment on the X-axis. The error bars represent the standard error of the mean. Relative fluorescence is expressed in quinine sulfate units (QSU).

For the *P. bahamense* bioassay, reductions of 34% and 17% for C1-humic were only observed in the Clearwater and Safety Harbor treatments, respectively (Table 2). These reductions were concomitant with 206%, 190%, and 47% increases for Control, Rain Low, and Rain High treatments, respectively. Reductions in C2-microbial humic were only observed in controls (77%), with measured increases of 232%, 197%, 75%, and 214% for Rain Low, Rain High, Clearwater, and Safety Harbor treatments, respectively. Reductions in C3-protein were only observed in the Clearwater treatment (32%), but increases of 24%,

451%, 809%, and 22% for Control, Rain Low, and Rain High, and Safety Harbor treatments were observed, respectively.

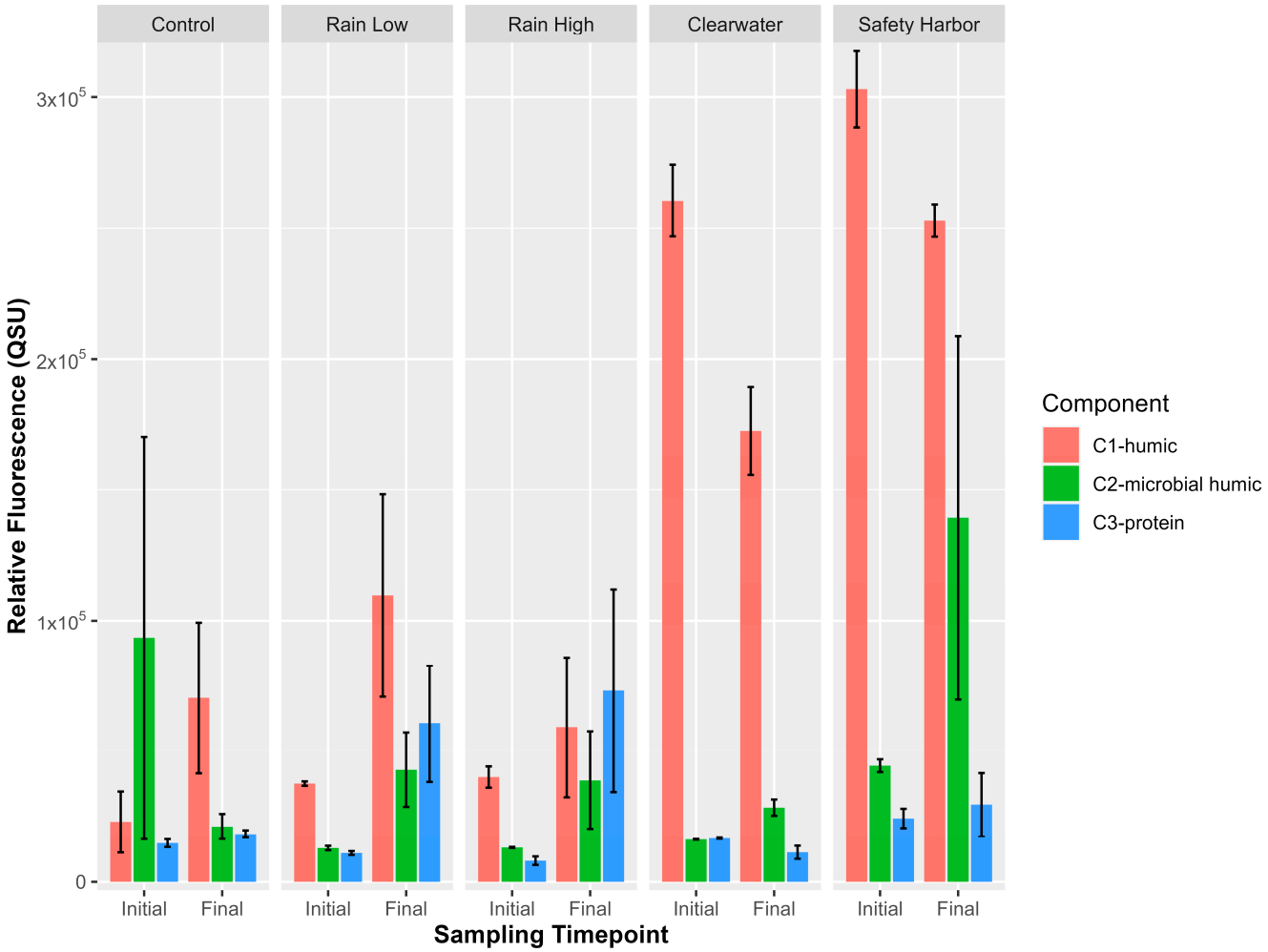

Figure 5. Changes in the relative fluorescence of FDOM components for the *P. bahamense* bioassay. The colored bars represent individual components, with comparisons between initial and final sampling timepoints for each treatment on the X-axis. The error bars represent the standard error of the mean. Relative fluorescence is expressed in quinine sulfate units (QSU).

Table 2. Percentage reduction in each FDOM component generated by PARAFAC model BIO-MOD. Calculations are based on change in relative fluorescence between initial and final timepoints per treatment for each bioassay. Negative values indicate an increase in fluorescence.

Bioassay	Sample ID	C1-Humic	C2-Microbial Humic	C3-Protein
K. brevis	Control	−12	100	75
	Rain Low	−6	98	59
	Rain High	4	96	−16
	Beachside	42	−8	−3995
	Mainland	25	35	20
P. bahamense	Control	−206	77	−24
	Rain Low	−190	−232	−451
	Rain High	−47	−197	−809
	Clearwater	34	−75	32
	Safety Harbor	17	−214	−22

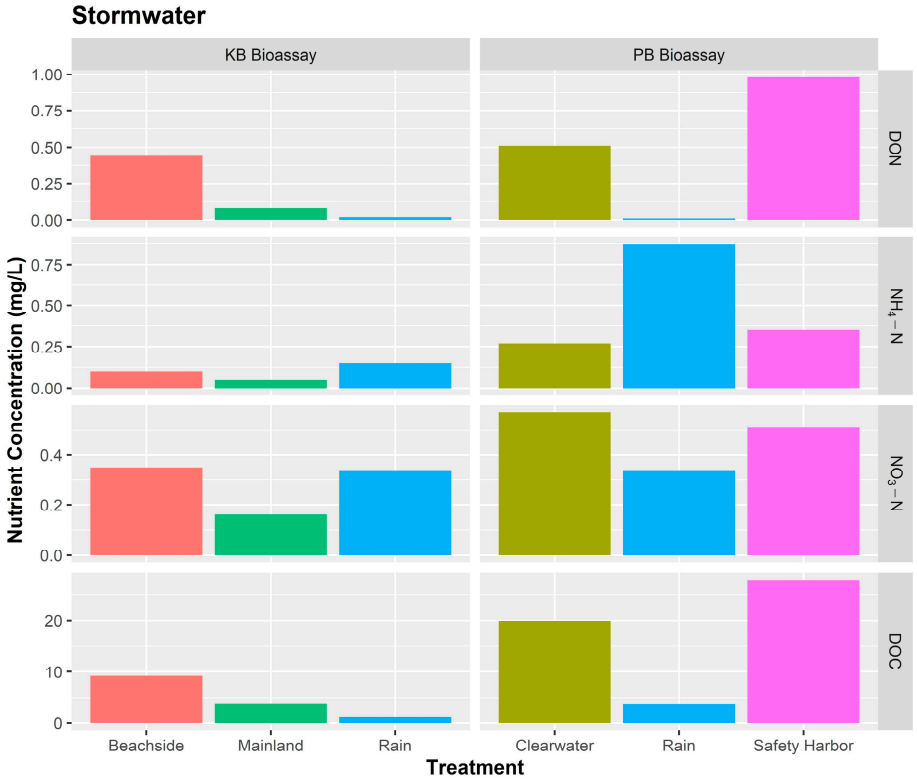

Figure 6. Concentrations of nitrogen forms (dissolved organic nitrogen = DON) and dissolved organic carbon (DOC) for the stormwater and rainfall used as inocula for both bioassays. Each stormwater or rainfall treatment collected for the respective bioassay is defined on the X-axis. Note the differences in axes and scales.

3.3. Fluorescence and UV Indices

The fluorescence and UV indices exhibited changes in FDOM and CDOM when comparing initial and final timepoints for each species (Table 3). For the *K. brevis* bioassay, the aromaticity of CDOM calculated using $SUVA_{254}$ remained relatively unchanged. HIX values increased for Control and Rain Low treatments, and decreased for the remaining treatments, suggesting the removal of humified material in the Rain High and stormwater treatments. BIX values decreased slightly in controls and remained unchanged in the Beachside treatments. Conversely, BIX values increased in all remaining treatments, indicating the production of autochthonous FDOM.

Table 3. The mean fluorescence and UV parameters, HIX (humification index), BIX (biological index), and $SUVA_{245}$ (specific ultraviolet absorption at 254 nm) of FDOM in the bioassay samples, comparing the initial and final timepoints for each treatment. The asterisk next to Sample ID represents pure stormwater and rainfall samples measured prior to inoculation which had no Final timepoint, as noted NA.

		HIX		BIX		$SUVA_{254}$ (L mg C^{-1} m^{-1})	
Bioassay	**Sample ID**	**Initial**	**Final**	**Initial**	**Final**	**Initial**	**Final**
K. brevis	Rainfall *	0.52	NA	0.73	NA	0.01	NA
	Beachside *	0.87	NA	0.57	NA	0.03	NA
	Mainland *	0.91	NA	0.56	NA	0.03	NA
	Control	0.79	0.86	1.32	1.28	0.01	0.01
	Rain Low	0.84	0.86	1.28	1.31	0.01	0.01
	Rain High	0.84	0.81	1.26	1.29	0.01	0.01
	Beachside	0.92	0.85	0.92	0.92	0.01	0.02
	Mainland	0.87	0.86	0.95	1.05	0.01	0.01

Table 3. *Cont.*

		HIX		BIX		$SUVA_{254}$ ($L\ mg\ C^{-1}\ m^{-1}$)	
Bioassay	**Sample ID**	**Initial**	**Final**	**Initial**	**Final**	**Initial**	**Final**
P. bahamense	Rainfall *	0.55	NA	0.84	NA	0.02	NA
	Clearwater *	0.88	NA	0.64	NA	0.03	NA
	Safety Harbor *	0.88	NA	1.10	NA	0.02	NA
	Control	0.59	0.67	1.25	1.11	0.01	0.05
	Rain Low	0.70	0.61	1.4	1.04	0.01	0.08
	Rain High	0.74	0.49	1.38	1.08	0.01	0.05
	Clearwater	0.87	0.86	0.75	0.77	0.02	0.02
	Safety Harbor	0.86	0.84	0.72	0.76	0.02	0.03

For the *P. bahamense* bioassay, the aromaticity of CDOM calculated using $SUVA_{254}$ slightly increased in Control, Rain Low, and Rain High treatments, indicating the production of CDOM with greater aromaticity; however, these values are still very low, indicative of predominantly aliphatic DOM. Conversely, $SUVA_{254}$ remained relatively unchanged for stormwater treatments. HIX values decreased in all treatments except for controls, suggesting the removal of humified FDOM in the rainfall and stormwater treatments. BIX values decreased in Control and rainfall treatments. Conversely, BIX values increased in both stormwater treatments, indicating the production of autochthonous FDOM.

3.4. Changes in Nitrogen Species and DOC

For both bioassays, stormwater runoff contributed the highest concentrations of DON and DOC (Figure 6). Conversely, rainfall contributed the most NH_4-N. For the *K. brevis* bioassay, reductions in DON were observed across all treatments until T_{72} (Figure 7). A preference for NH_4-N was observed as opposed to NO_3-N, and NO_3-N concentrations remained relatively unchanged. DOC steadily decreased until the final timepoint (T_{120}) across all treatments.

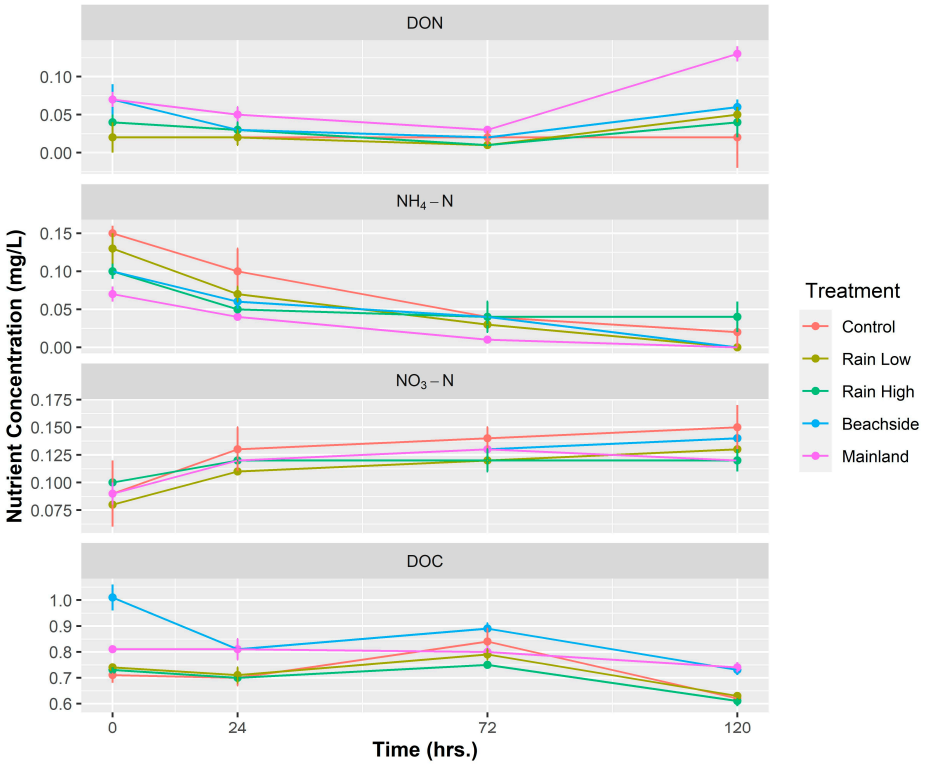

Figure 7. Change in concentrations of nitrogen forms (dissolved organic nitrogen = DON) and dissolved organic carbon (DOC) vs. time for the *K. brevis* bioassay. Colored lines represent individual

rainfall or stormwater treatments. Error bars represent standard error of mean. Note differences in Y-axes.

For the *P. bahamense* bioassay, a complete drawdown of DON was observed in 48 h for all treatments, except controls (Figure 8). Like *K. brevis*, a preference for NH_4-N was observed as opposed to NO_3-N, as values for NH_4-N steadily declined until T_{96}. NH_4-N increased until the final timepoint (T_{144}), which was concomitant with decreases in DOC.

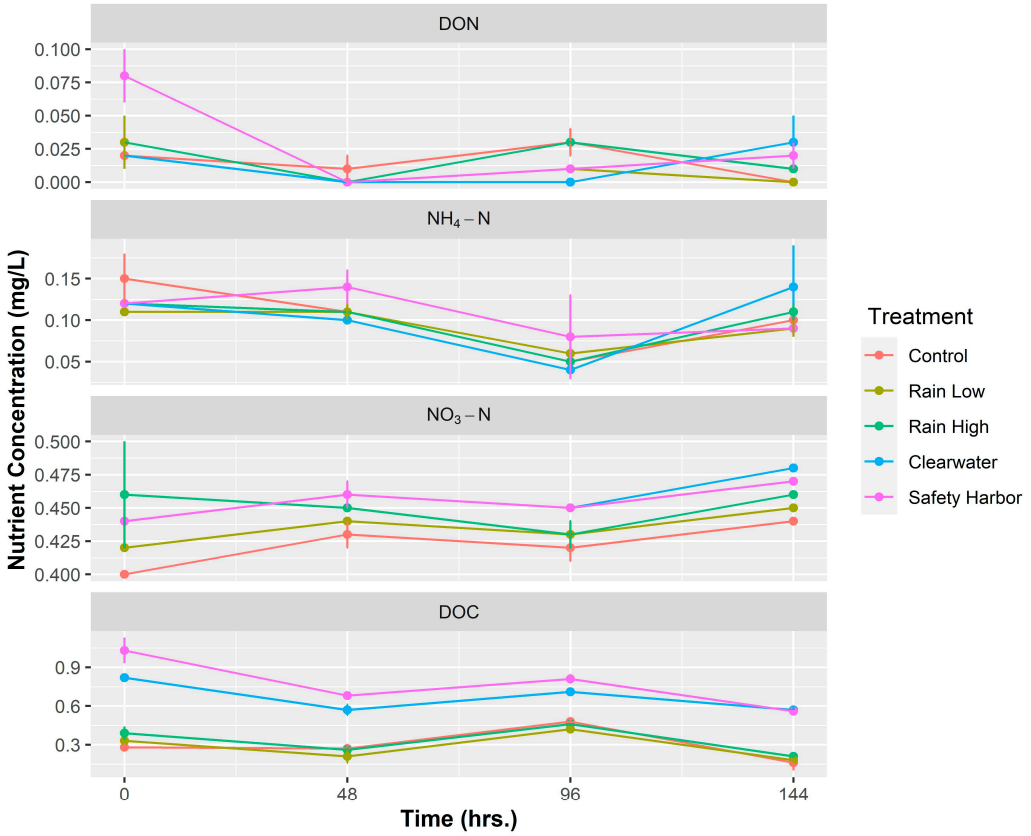

Figure 8. Change in concentrations of nitrogen forms (dissolved organic nitrogen = DON) and dissolved organic carbon (DOC) vs. time for the *P. bahamense* bioassay. Colored lines represent individual rainfall or stormwater treatments. Error bars represent standard error of mean. Note differences in Y-axes.

To determine the bioavailable DON (BDON) fraction within each stormwater treatment, BDON was calculated using the difference of the mean initial and mean DON concentrations at T_{72} for *K. brevis* and T_{48} for *P. bahamense*, and the percentage of BDON was calculated by dividing BDON by the initial mean DON × 100 (Table 4). These timepoints were chosen due to the observed depletion in DON, which was followed by the subsequent production of DON. For the *K. brevis* bioassay, BDON was 75%, 71%, 57%, and 50% for the Rain High, Beachside, Mainland, and Rain Low treatments, respectively. BDON was 100% for all treatments in the *P. bahamense* bioassay except for controls.

The same calculation was performed to measure bioavailable DOC (BDOC), using initial (T_0) and final timepoints (T_{120} for *K. brevis*; T_{144} for *P. bahamense*) (Table 4). BDOC was greatest for the Beachside treatment (28%) and lowest for the Mainland (9%) treatment for the *K. brevis* bioassay, indicating Mainland DOC was more recalcitrant. This pattern was despite relatively equal contributions of terrestrial and soil fulvic-like DOM. The greatest BDOC was equal for Rain High and Safety Harbor (46%) for the *P. Bahamense* bioassay, and lowest for the Clearwater treatment (30%). Clearwater FDOM had relatively equal contributions of terrestrial and soil fulvic-like DOM, whereas rainfall and Safety Harbor

FDOM was predominantly humic-like (98 and 72%, respectively) (Figure 9). Further, Safety Harbor source water had greater DOC concentrations and the relative fluorescence of SW1-terrestrial humic was almost double that of Clearwater, indicating that the response may have been due to the dose rather than the bioavailability of DOM.

Table 4. Percentage of bioavailable dissolved organic nitrogen (%BDON) and percentage of bioavailable dissolved organic carbon (%BDOC) for each bioassay. %BDON was calculated using hours 0 and 72 and hours 0 and 48 for *K. brevis* and *P. bahamense* bioassays, respectively.

Bioassay	Sample ID	%BDON	%BDOC
K. brevis	Control	0	13
	Rain Low	50	15
	Rain High	75	16
	Beachside	71	28
	Mainland	57	9
P. bahamense	Control	50	43
	Rain Low	100	45
	Rain High	100	46
	Clearwater	100	30
	Safety Harbor	100	46

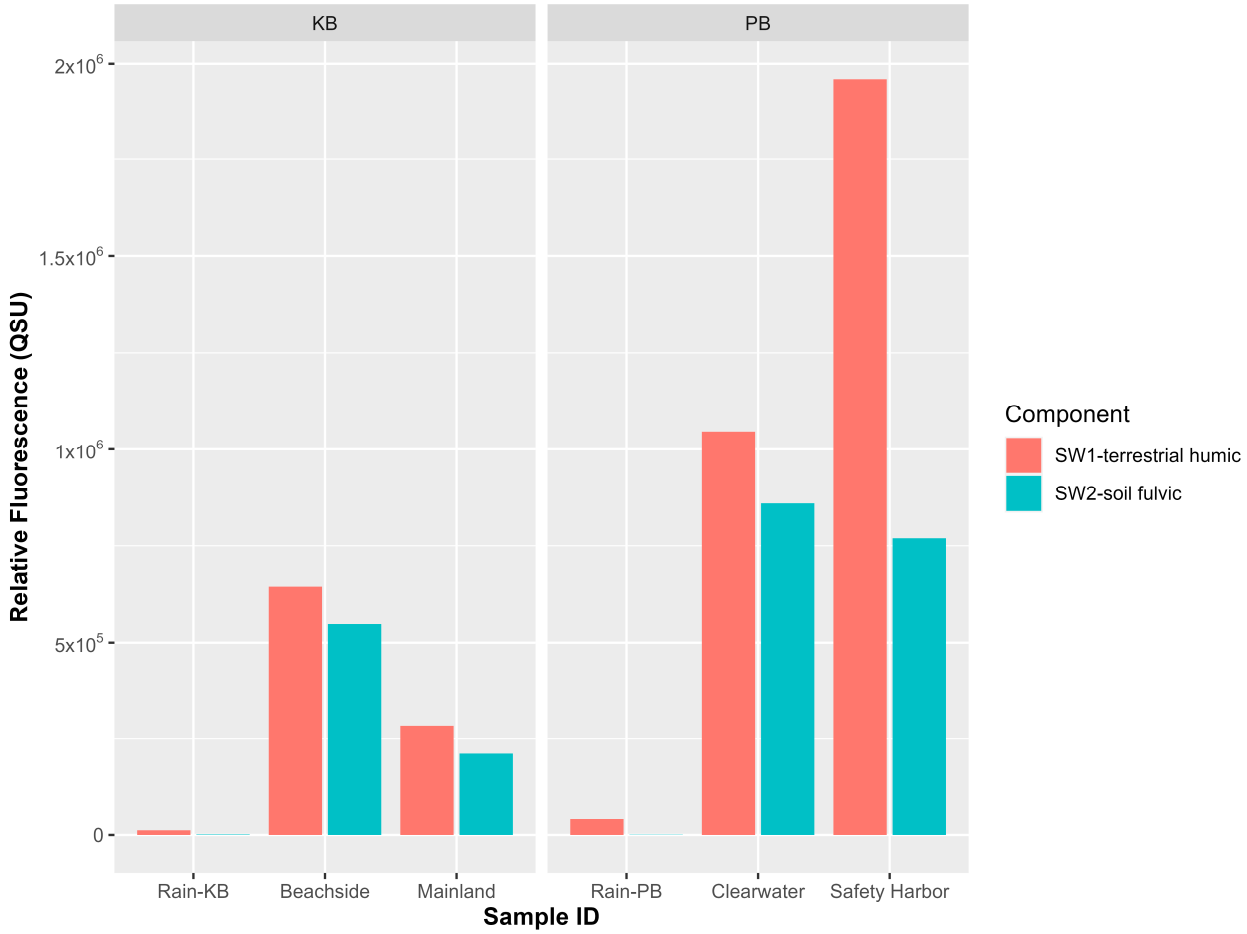

Figure 9. Relative fluorescence of components for stormwater runoff and rainfall used as inocula for *K. brevis* (KB) and *P. bahamense* (PB) bioassays. Colored bars represent individual components generated from PARAFAC model. SW1 represents terrestrial humic-like FDOM. Each stormwater or rainfall treatment collected for the respective bioassay is defined on the X-axis. Relative fluorescence is expressed in quinine sulfate units (QSU).

3.5. Growth Response

For the *K. brevis* bioassay, significant differences in maximum cell concentrations were measured in the Mainland and Beachside treatments (Table 5, Figure 10). Mainland mean maximum cell concentrations were the highest overall ($5.9 \times 10^5 \pm 1.1 \times 10^5$ cells L^{-1}) and significantly greater than all other treatments, including controls ($p \leq 0.0001$). The specific growth rate for the Mainland treatment was $\mu = 0.52 \pm 0.05$ day $^{-1}$, which was only slightly significant when compared to controls ($p = 0.08$). This growth rate was the same for the High Rain treatment; however, the maximum cell concentrations were almost two-fold greater for the Mainland treatment.

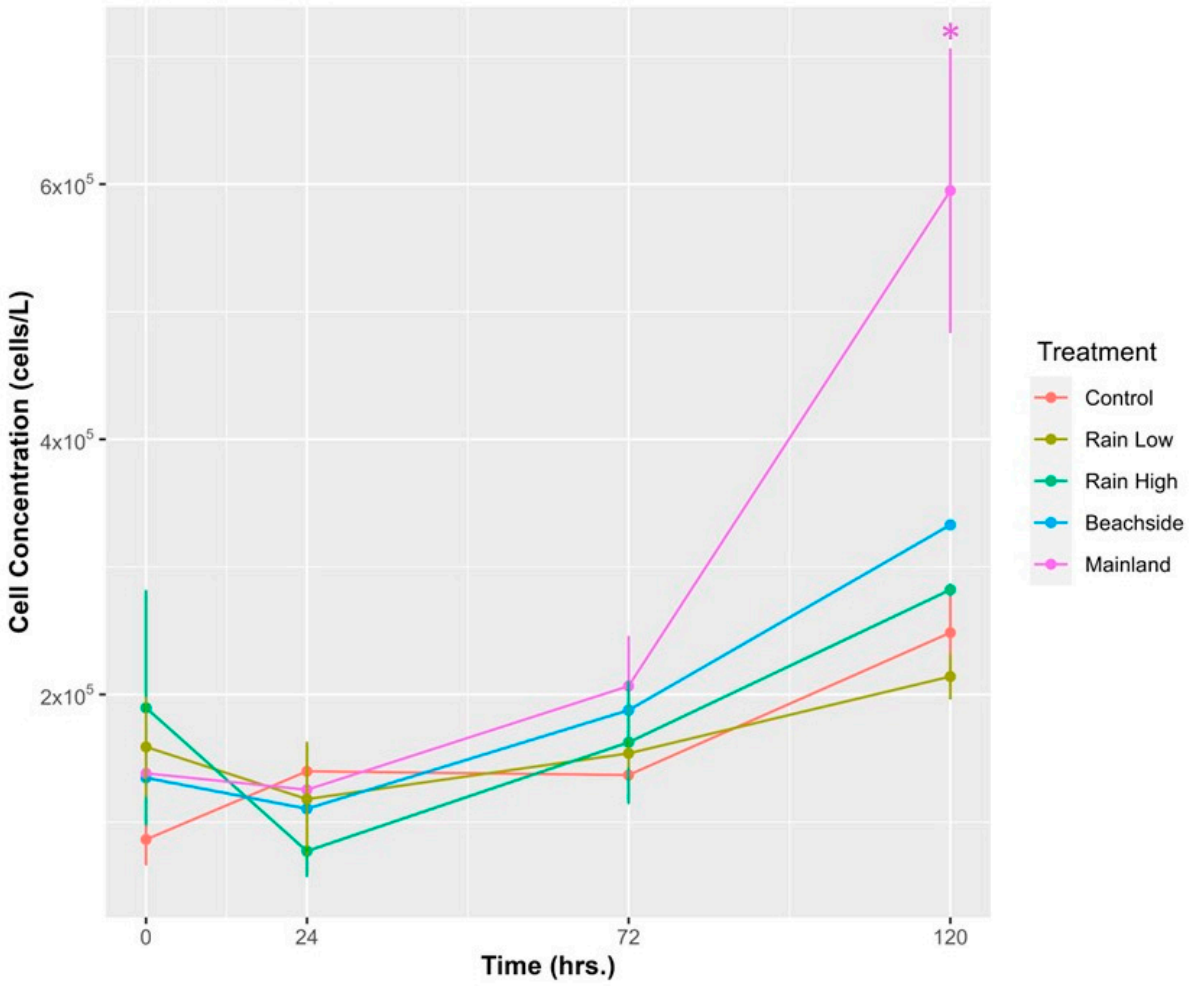

Figure 10. *Karenia brevis* cell concentrations vs. time in hours. Colored lines represent individual rainfall or stormwater treatments. Error bars represent standard error of mean. Colored asterisk denotes statistical significance of maximum cell concentrations vs. Control treatment ($p \leq 0.05$).

Beachside maximum cell concentrations ($3.3 \times 10^5 \pm 3.6 \times 10^3$ cells L^{-1}) were significantly greater than the Rain Low treatment ($p = 0.02$) and only slight significance was observed when compared to controls ($p = 0.12$). Beachside growth rates ($\mu = 0.63 \pm 0.21$ day $^{-1}$) were also significantly greater than controls ($p < 0.005$), which were the highest across all treatments. All treatments had a lag time of 24 h, with the exception of controls (0 h).

For the *P. bahamense* bioassay, significant differences in maximum cell concentrations were measured in Clearwater ($p = 0.05$), Safety Harbor ($p = 0.01$), and Rain High ($p = 0.003$) treatments when compared to controls (Table 5, Figure 11). Rain High and Safety Harbor were also significantly greater than Rain Low ($p = 0.01$ and $p = 0.05$, respectively). Specific growth rates for the Clearwater treatment were significantly greater than controls ($p = 0.01$),

measured at $\mu = 1.45 \pm 0.39$ day $^{-1}$. Specific growth rates for all remaining treatments were greater compared to controls in the order of Rain Low < Rain High < Safety Harbor. All treatments had zero lag time, with the exception of the Control and Safety Harbor treatments (24 h).

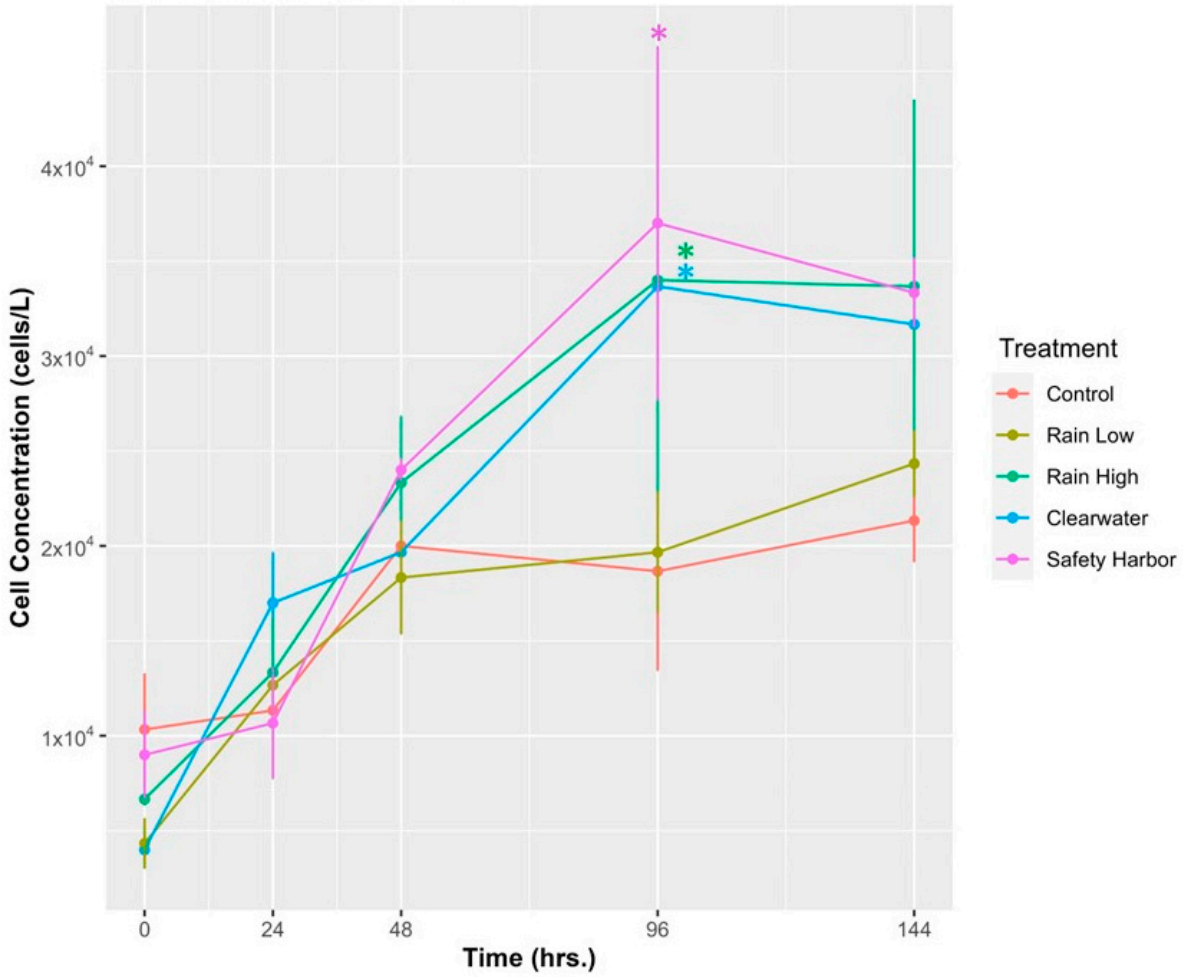

Figure 11. *Pyrodinium bahamense* cell concentrations vs. time in hours. Colored lines represent individual rainfall or stormwater treatments. Error bars represent standard error of mean. Colored asterisk denotes statistical significance of maximum cell concentrations vs. Control treatment ($p \leq 0.05$).

Table 5. Mean specific growth rates in divisions per day, mean maximum cell concentrations, and lag time for each bioassay and sample type. Values are ± standard error of mean.

Bioassay	Sample ID	Division Rate, μ (day $^{-1}$)	Maximum Cell Concentration (cells L^{-1})	Lag Time (h)
K. brevis	Control	0.29 (±0.02)	2.5×10^5 ($\pm 3.7 \times 10^4$)	0
	Rain Low	0.34 (±0.07)	2.3×10^5 ($\pm 1.4 \times 10^4$)	24
	Rain High	0.52 (±0.05)	3.1×10^5 ($\pm 2.7 \times 10^4$)	24
	Beachside	0.63 (±0.21)	3.3×10^5 ($\pm 3.6 \times 10^3$)	24
	Mainland	0.52 (±0.05)	5.9×10^5 ($\pm 1.1 \times 10^5$)	24
P. bahamense	Control	0.53 (±0.14)	2.4×10^4 ($\pm 2.1 \times 10^3$)	24
	Rain Low	1.01 (±0.28)	2.4×10^4 ($\pm 6.7 \times 10^2$)	0
	Rain High	0.92 (±0.20)	3.4×10^4 ($\pm 9.3 \times 10^3$)	0
	Clearwater	1.45 (±0.39)	3.4×10^4 ($\pm 3.5 \times 10^3$)	0
	Safety Harbor	0.89 (±0.26)	3.7×10^4 ($\pm 7.1 \times 10^3$)	24

4. Discussion

The bioassay results and EEM-PARAFAC analysis demonstrate that stormwater inputs support *K. brevis* and *P. bahamense* growth by providing labile FDOM predominantly in the form of allochthonous humic substances and DON. These results support previous studies that have shown that *K. brevis* can utilize humic and DON compounds for growth [25,76]. While direct uptake of humic substances have not been investigated for *P. bahamense*, it can be speculated that humic substances likely play a role in bloom proliferation as the addition of soil extracts [39] to cultures and mangrove leaf leachate added to natural bloom populations [77] in previous studies resulted in an increase in biomass. Autochthonous humic- and protein-like FDOM were either refractory or produced as a byproduct of consumption of bioavailable FDOM and/or inorganic nutrients (notably, NH_4-N). Both rainfall and runoff additions elicited a faster growth rate for *K. brevis* and *P. bahamense*, indicating that these inputs can potentially lead to bloom expansion.

Both *K. brevis* and *P. bahamense* exhibited the greatest growth response measured as the maximum cell concentration for each stormwater runoff treatment and simulated high rainfall treatment compared to controls. This indicates that stormwater runoff and rainfall contribute bioavailable FDOM, as well as NH_4-N, which contributed to this increase in biomass. Interestingly, the specific growth rate, BDON, and BDOC were lower for the Mainland treatment vs. the Rainfall High and Beachside treatments. However, the maximum cell concentrations were almost two-fold greater for the Mainland treatment. These results mirror the growth response of *K. brevis* cultures in a previous study by Muni-Morgan et al. [76], where younger stormwater pond (14 yrs) and wastewater effluent additions had the highest pools of BDON and growth rates, while the effluent from the older pond effluent (18–34 yrs.) yielded the highest maximum cell concentration (~2.7×10^6 cells L^{-1}) despite having lower BDON/growth rates. These results suggest that DOM and nutrient sources such as aged stormwater pond effluent and mainland runoff may contain more biorefractory DOM (i.e., humic acids) that can result in lower growth rates, but can sustain slow, long-term growth.

Changes in the relative fluorescence of components comparing initial and final timepoints indicate greater reactivity of stormwater FDOM, specifically terrestrial humic-like C1. Despite this component observed in controls, we can conclude that the C1-humic utilized was terrestrial in origin for stormwater treatments due to the contribution of C1-humic from the source water (Figure 9), as well as the greater HIX values and lower BIX values observed at T_0 in the stormwater treatments vs. controls (Table 3).

Both *K. brevis* and *P. bahamense* prefer reduced forms of N. By hour 48, 100% of the DON in each treatment was utilized by *P. bahamense.* By hour 72, over 50% of the DON was utilized by *K. brevis*, except for controls, corresponding with an increase in cell concentrations. These results indicate that the added DON from runoff and rainfall was highly bioavailable. Unfortunately, T_{48} and T_{72} were not included in the EEM analysis, and we were unable to identify which FDOM components were depleted. DON may be more preferred by *P. bahamense* than *K. brevis*, as reductions in DON preceded reductions in NH_4-N at T_{96}, indicating a preference for DON, followed by NH_4-N when DON subsidies are depleted. No clear preference for NO_3-N was observed for both species, suggesting a lower affinity compared to DON and NH_4-N. These results are in line with previous studies observing preferential uptake of chemically reduced (NH_4^+) vs. oxidized (NO_3^-) N forms by phytoplankton ([78] and references therein). However, this is in conflict with previous research suggesting laboratory cultures of *P. bahamense* prefer NO_3-N for growth [39].

For *K. brevis*, depletions in NH_4-N were concomitant with the production of DON. However, all FDOM components decreased in relative fluorescence at the final timepoint. Algae are known to produce DON as they assimilate inorganic N [79], and these results suggest that the N compounds exuded during growth were non-fluorescent and potentially composed of unsaturated organic compounds [74]. These could include non-fluorescing carbohydrate molecules [80]. For example, the N-limited status of phytoplankton has been shown to cause the release of organic substances such as polysaccharides, which

can make up 80–90% of algal exudates [81]. Carbohydrates are typically devoid of N; however, marine algae possess storage products such as mucopolysaccharides which do contain N [82].

The calculations of BDOC were greater for the *P. bahamense* bioassay compared to *K. brevis* (30–46% vs. 9–28%, respectively). This suggests that DOC is preferred by *P. bahamense* compared to *K. brevis*; however, the concentrations of DOC in the source water were almost two-fold that which were added to *K. brevis* (Figure 6). Further, BIX was higher for the stormwater runoff added to *P. bahamense* cultures vs. *K. brevis*, indicating that these sites conveyed more humic-like DOM of recent microbial origin, which may have played a role in increased lability. The reduction in DOC during both bioassays for the stormwater treatments was concomitant with the reduction in humic-like C1 (Peak A + C). Conversely, C1-humic increased in all other treatments (apart from Rain High for *K. brevis*), indicating that *P. bahamense* and *K. brevis* exudates can share spectral characteristics with those of terrestrial humic material, which could be due to increased aromaticity and polycondensation [83]. This is confirmed by the increase in $SUVA_{254}$ values and/or HIX, which indicates a production of FDOM that is more aromatic, and/or preferential consumption of aliphatic, non-aromatic DOM [63]. The production of humic peak C has also been documented in other phytoplankton incubation experiments [75,84], highlighting the role that phytoplankton play in the production of biorefractory humic materials.

C2-microbial humic increased in all treatments except controls for *P. bahamense*, and C3-protein increased across all treatments except for the Clearwater treatment. This indicates that pulses of rainfall and/or runoff can result in autochthonous production of microbial humic-like and protein-like FDOM. It is noteworthy that C2-microbial humic decreased in controls, indicating the capability of *P. bahamense* to recycle autochthonous humic substances if nutrient limitation, namely DON, occurs. Similar patterns of C2-microbial humic were observed for *K. brevis*, as C2-microbial humic was reduced in controls and both rainfall treatments but remained relatively unchanged in stormwater treatments, indicating a preference for allochthonous humic FDOM.

For *K. brevis*, C3 protein-like fluorescence decreased the most in controls and the Rain Low treatment, which could also indicate the recycling of tyrosine-like FDOM. Conversely, tyrosine-like FDOM increased by four orders of magnitude in the Beachside treatment, concomitant with increases in DON, which suggests exudation of proteins during the utilization of allochthonous humic-like FDOM. The greater release of DON observed due to additions of stormwater has implications for bloom maintenance over longer time scales, as regenerated DON produced *in situ* can be recycled [22,85]. Further, autochthonous production of FDOM due to atmospheric and stormwater inputs has implications for the microbial loop [86]. For example, bacterial cycling of DON may be intensified due to releases of labile DON in N-limited conditions, which can effect planktonic community composition and energy supply to higher trophic levels [87]. We also emphasize that both cultures of *K. brevis* and *P. bahamense* were non-axenic, and a reduction/increase in DOM fluorescence may be due to bacterial consumption/production of FDOM compounds; this relationship should be investigated further.

For *K. brevis*, the maximum cell concentrations were similar for Control and Rain Low treatments, indicating that 1 cm of rainfall may not result in increased biomass in natural bloom populations. Conversely, 4 cm rainfall events and inputs of stormwater from mainland sources can result in up to a two-fold increase in biomass. This increase due to runoff has ecological, human health, and management implications. For example, in the state of Florida, the *K. brevis* concentration threshold for shellfish bed closures is 5×10^3 cells L^{-1} [88]. Further, fish kills can occur at *K. brevis* concentrations $> 5 \times 10^4$ cells L^{-1} [88], which can result in subsequent hypoxia [89]. Likewise, human health risks due to aerosolized brevetoxins increase with bloom expansion, as respiratory irritation can occur at *K. brevis* concentrations as low as 1×10^3 cells L^{-1} [88], with increasing severity as concentrations exceed 1×10^6 cells L^{-1} [90].

Similarly, ecological, human health, and management implications exist for allochthonous inputs in blooms of *P. bahamense*, as both rainfall doses and stormwater treatments resulted in increased cell yields vs. controls. For example, shellfish bed closures occur when saxitoxin levels are ≥80 µg/100g of shellfish tissue [91], and blooms in excess of 1×10^5 cells L^{-1} can reduce water column light penetration, negatively impacting seagrass beds [92]. Bloom concentrations can also deplete oxygen within the water column, resulting in fish kills [93].

5. Conclusions

This study highlights the utility of EEM spectroscopy for analysis of DOM in algal bioassay studies, providing a tool to track DOM transformation and utilization. Both *K. brevis* and *P. bahamense* contribute to the production of humic-like DOM in estuarine and coastal waters. The existing criteria for distinguishing terrestrial allochthonous sources of humic-like DOM (e.g., peak A + C in C1-humic) should be further resolved due to the measured production of this fluorophore in controls of both *K. brevis* and *P. bahamense*. Further research using optical proxies (i.e., HIX and BIX) is needed to identify humic-like material produced by HABs when monitoring DOM with EEM-PARAFAC, as this component can be misinterpreted as terrestrial humic material supporting blooms rather than that which is produced *in situ*.

In conclusion, bloom management should be inclusive of stormwater management, including monitoring the export and chemical characteristics of DOM, DON, as well as NH_4-N loads during storm events to mitigate the associated ecological and human health risks of *K. brevis* and *P. bahamense* blooms. Future research investigating the response of natural bloom populations to these inputs is needed to fully constrain the roles of rainfall and runoff from urban land use in supporting blooms, as the affinity of labile fractions of DOM are not equal across species. Further, spatial and chemical variations exist for allochthonous inputs entering Tampa Bay waters.

Author Contributions: Conceptualization, methodology, formal analysis, investigation, data curation, visualization, and writing—original draft preparation, A.L.M.-M.; resources and writing—review and editing, M.G.L. and C.A.H.; project administration and funding acquisition, M.G.L. All authors have read and agreed to the published version of the manuscript.

Funding: This research was partially funded by a grant from the Tampa Bay Estuary Program through their Tampa Bay Environmental Restoration Fund. We also acknowledge support from the University of Florida Center for Land Use Efficiency. This paper is a result of research funded by the National Oceanic and Atmospheric Administration National Centers for Coastal Ocean Science Competitive Research Program under award NA19NOS4780183. This is ECOHAB publication number 1099.

Data Availability Statement: The original data presented in this study are openly available in the KNB repository at https://knb.ecoinformatics.org/view/urn:uuid:a2626104-f8bd-4ac1-a5d1-33c71d8c1499 (accessed on 1 April 2024).

Acknowledgments: We express gratitude to the Red Tide Institute at Mote Marine Laboratory for providing *K. brevis* cultures, supplies, and incubation space, as well as assistance from Sarah Klass in maintaining the cultures. We also thank Carey Lopez and Katherine Hubbard at the Florida Fish and Wildlife Research Institute for providing *P. bahamense* cultures and for their helpful insight. We thank Paula Sanchez Garzon for assisting in the bioassay setup and sample processing, and Salvatore Caprara of the University of South Florida for providing access to the Horiba Aqualog. We also thank Rasmus Bro for providing helpful guidance and expertise on PARAFAC analysis.

Conflicts of Interest: The authors declare no conflicts of interest.

References

1. Howarth, R.W.; Sharpley, A.; Walker, D. Sources of nutrient pollution to coastal waters in the United States: Implications for achieving coastal water quality goals. *Estuaries* **2002**, *25*, 656–676. [CrossRef]
2. Anderson, D.M.; Glibert, P.M.; Burkholder, J.M. Harmful algal blooms and eutrophication: Nutrient sources, composition, and consequences. *Estuaries* **2002**, *25*, 704–726. [CrossRef]

3. Smith, M.A.; Kominoski, J.S.; Gaiser, E.E.; Price, R.M.; Troxler, T.G. Stormwater runoff and tidal flooding transform dissolved organic matter composition and increase bioavailability in urban coastal ecosystems. *J. Geophys. Res. Biogeosci.* **2021**, *126*, e2020JG006146. [CrossRef]
4. Chen, H.; Liao, Z.-L.; Gu, X.-Y.; Xie, J.-Q.; Li, H.-Z.; Zhang, J. Anthropogenic Influences of Paved Runoff and Sanitary Sewage on the Dissolved Organic Matter Quality of Wet Weather Overflows: An Excitation-Emission Matrix Parallel Factor Analysis Assessment. *Environ. Sci. Technol.* **2017**, *51*, 1157–1167. [CrossRef]
5. Sipler, R. The Role of Dissolved Organic Matter in Structuring Microbial Community Composition. Ph.D. Thesis, New Brunswick Rutgers, The State University of New Jersey, New Brunswick, NJ, USA, 2009.
6. Seitzinger, S.P.; Sanders, R.W. Atmospheric inputs of dissolved organic nitrogen stimulate estuarine bacteria and phytoplankton. *Limnol. Oceanogr.* **1999**, *44*, 721–730. [CrossRef]
7. Petrone, K.C.; Fellman, J.B.; Hood, E.; Donn, M.J.; Grierson, P.F. The origin and function of dissolved organic matter in agro-urban coastal streams. *J. Geophys. Res.* **2011**, *116*, G1. [CrossRef]
8. Bianchi, T.S. *Biogeochemistry of Estuaries*; Oxford University Press: Oxford, UK, 2006; ISBN 9780195160826.
9. D'Andrilli, J.; Cooper, W.T.; Foreman, C.M.; Marshall, A.G. An ultrahigh-resolution mass spectrometry index to estimate natural organic matter lability. *Rapid Commun. Mass Spectrom.* **2015**, *29*, 2385–2401. [CrossRef]
10. Hopkinson, C.S.; Buffam, I.; Hobbie, J.; Vallino, J.; Perdue, M.; Eversmeyer, B.; Prahl, F.; Covert, J.; Hodson, R.; Moran, M.A.; et al. Terrestrial inputs of organic matter to coastal ecosystems: An intercomparison of chemical characteristics and bioavailability. *Biogeochemistry* **1998**, *43*, 211–234. [CrossRef]
11. Bianchi, T.S. The role of terrestrially derived organic carbon in the coastal ocean: A changing paradigm and the priming effect. *Proc. Natl. Acad. Sci. USA* **2011**, *108*, 19473–19481. [CrossRef]
12. McElmurry, S.P.; Long, D.T.; Voice, T.C. Stormwater dissolved organic matter: Influence of land cover and environmental factors. *Environ. Sci. Technol.* **2014**, *48*, 45–53. [CrossRef]
13. Huguet, A.; Vacher, L.; Relexans, S.; Saubusse, S.; Froidefond, J.M.; Parlanti, E. Properties of fluorescent dissolved organic matter in the Gironde Estuary. *Org. Geochem.* **2009**, *40*, 706–719. [CrossRef]
14. Stedmon, C.A.; Bro, R. Characterizing dissolved organic matter fluorescence with parallel factor analysis: A tutorial. *Limnol. Oceanogr. Methods* **2008**, *6*, 572–579. [CrossRef]
15. Coble, P.; Lead, J.; Baker, A.; Reynolds, D.M.; Spencer, R.G.M. (Eds.) *Aquatic Organic Matter Fluorescence*; Cambridge University Press: Cambridge, UK, 2014; ISBN 9781139045452.
16. Bro, R. PARAFAC. Tutorial and applications. *Chemom. Intell. Lab. Syst.* **1997**, *38*, 149–171. [CrossRef]
17. Bro, R.; Viereck, N.; Toft, M.; Toft, H.; Hansen, P.I.; Engelsen, S.B. Mathematical chromatography solves the cocktail party effect in mixtures using 2D spectra and PARAFAC. *TrAC Trends Anal. Chem.* **2010**, *29*, 281–284. [CrossRef]
18. Fleming, L.E.; Kirkpatrick, B.; Backer, L.C.; Bean, J.A.; Wanner, A.; Dalpra, D.; Tamer, R.; Zaias, J.; Cheng, Y.S.; Pierce, R.; et al. Initial evaluation of the effects of aerosolized Florida red tide toxins (brevetoxins) in persons with asthma. *Environ. Health Perspect.* **2005**, *113*, 650–657. [CrossRef]
19. Steidinger, K.A. Historical perspective on *Karenia brevis* red tide research in the Gulf of Mexico. *Harmful Algae* **2009**, *8*, 549–561. [CrossRef]
20. Steidinger, K.A. Implications of dinoflagellate life cycles on initiation of *Gymnodinium breve* red tides. *Environ. Lett.* **1975**, *9*, 129–139. [CrossRef]
21. Baden, D.G.; Mende, T.J. Amino acid utilization by *Gymnodinium breve*. *Phytochemistry* **1979**, *18*, 247–251. [CrossRef]
22. Heil, C.A.; Dixon, L.K.; Hall, E.; Garrett, M.; Lenes, J.M.; O'Neil, J.M.; Walsh, B.M.; Bronk, D.A.; Killberg-Thoreson, L.; Hitchcock, G.L.; et al. Blooms of *Karenia brevis* (Davis) G. Hansen & Ø. Moestrup on the West Florida Shelf: Nutrient sources and potential management strategies based on a multi-year regional study. *Harmful Algae* **2014**, *38*, 127–140. [CrossRef]
23. Killberg-Thoreson, L.; Sipler, R.E.; Heil, C.A.; Garrett, M.J.; Roberts, Q.N.; Bronk, D.A. Nutrients released from decaying fish support microbial growth in the eastern Gulf of Mexico. *Harmful Algae* **2014**, *38*, 40–49. [CrossRef]
24. Mendoza, W.G.; Kang, Y.; Zika, R.G. Resolving DOM fluorescence fractions during a *Karenia brevis* bloom patch on the Southwest Florida Shelf. *Cont. Shelf Res.* **2012**, *32*, 121–129. [CrossRef]
25. Killberg-Thoreson, L.; Mulholland, M.R.; Heil, C.A.; Sanderson, M.P.; O'Neil, J.M.; Bronk, D.A. Nitrogen uptake kinetics in field populations and cultured strains of *Karenia brevis*. *Harmful Algae* **2014**, *38*, 73–85. [CrossRef]
26. Meng, F.; Huang, G.; Yang, X.; Li, Z.; Li, J.; Cao, J.; Wang, Z.; Sun, L. Identifying the sources and fate of anthropogenically impacted dissolved organic matter (DOM) in urbanized rivers. *Water Res.* **2013**, *47*, 5027–5039. [CrossRef]
27. Rounsefell, G.A.; Nelson, W.R. *Red-Tide Research Summarized to 1964: Including an Annotated Bibliography*; U.S. Department of the Interior, Bureau of Commercial Fisheries: Washington, DC, USA, 1966; Volume 20.
28. Steidinger, K.A.; Burklew, M.A.; Ingle, R.M. The Effects of *Gymnodinium breve* Toxin on Estuarine Animals. In *Marine Pharmacognosy: Action of Marine Toxins at the Cellular Level*; Martin, D.F., Padilla, G.M., Eds.; Academic Press: New York, NY, USA, 1973; pp. 179–202.
29. Dixon, L.K.; Steidinger, K.A. Correlation of *Karenia brevis* presence in the eastern Gulf of Mexico with rainfall and riverine flow. In *Harmful Algae*; Steidinger, K.A., Landsberg, J.H., Tomas, C.R., Vargo, G.A., Eds.; Florida Fish and Wildlife Conservation Commission of UNESCO: Tallahassee, FL, USA, 2002; pp. 29–31.

30. Sobrinho, B.; Glibert, P.M.; Lyubchich, V.; Heil, C.A.; Li, M. Time series analysis of the *Karenia brevis* blooms on the West Florida Shelf: Relationships with El Niño—Southern Oscillation (ENSO) and its rate of change. In Proceedings of the 19th International Conference on Harmful Algae, La Paz, Mexico; 2022; pp. 232–237. [CrossRef]
31. Heil, C.A.; Muni-Morgan, A.L. Florida's harmful algal bloom (HAB) problem: Escalating risks to human, environmental and economic health with climate change. *Front. Ecol. Evol.* **2021**, *9*, 646080. [CrossRef]
32. Phlips, E.J.; Badylak, S.; Bledsoe, E.; Cichra, M. Factors affecting the distribution of *Pyrodinium bahamense* var. *bahamense* in coastal waters of Florida. *Mar. Ecol. Prog. Ser.* **2006**, *322*, 99–115. [CrossRef]
33. Shankar, S.; Lopez, C.; Kaminski, S.G.; Hubbard, K.A.; Flewelling, L. *Toxicity of Pyrodinium bahamense Cells and Resting Cysts in Tampa Bay, Florida*; Fish and Wildlife Research Institute: St. Petersburg, FL, USA, 2023.
34. Morquecho, L. *Pyrodinium bahamense* One the Most Significant Harmful Dinoflagellate in Mexico. *Front. Mar. Sci.* **2019**, *6*, 1. [CrossRef]
35. Lopez, C.; Smith, C.G.; Marot, M.; Karlen, D.; Karim, A.; Corcoran, A. *Pyrodinium bahamense Seeding Potential in Tampa Bay: Executive Summary*; Tampa Bay Estuary Program: St. Petersburg, FL, USA, 2020.
36. Lopez, C.B.; Shankar, S.; Kaminski, S.G.; Hubbard, K.A. *Pyrodinium bahamense Bloom Dynamics in Old Tampa Bay, FL, with a Focus on Feather Sound*; Florida Scientist: Saint Petersburg, FL, USA, 2023.
37. Karlen, D.; Campbell, K.W. The distribution of Pyrodinium bahamense cysts in Old Tampa Bay sediments. *Environ. Prot. Comm. Hillsoborough Cty* **2012**. [CrossRef]
38. Sherwood, E.T.; Greening, H.; Garcia, L.; Kaufman, K.; Janicki, T.; Pribble, R.; Cunningham, B.; Peene, S.; Fitzpatrick, J.; Dixon, K.; et al. Development of an integrated ecosystem model to determine effectiveness of potential watershed management projects on improving Old Tampa Bay. In *Headwaters to Estuaries: Advances in Watershed Science and Management, Proceedings of the Fifth Interagency Conference on Research in the Watersheds, North Charleston, SC, USA, 2–5 March 2015*; Stringer, C.E., Krauss, K.W., Latimer, J.S., Eds.; U.S. Department of Agriculture Forest Service, Southern Research Station: Asheville, NC, USA, 2016; p. 302.
39. Usup, G.; Ahmad, A.; Matsuoka, K.; Lim, P.T.; Leaw, C.P. Biology, ecology and bloom dynamics of the toxic marine dinoflagellate *Pyrodinium bahamense*. *Harmful Algae* **2012**, *14*, 301–312. [CrossRef]
40. Morquecho, L.; Alonso-Rodríguez, R.; Arreola-Lizárraga, J.A.; Reyes-Salinas, A. Factors associated with moderate blooms of *Pyrodinium bahamense* in shallow and restricted subtropical lagoons in the Gulf of California. *Bot. Mar.* **2012**, *55*, 611–623. [CrossRef]
41. Núñez-Vázquez, E.J.; Poot-Delgado, C.A.; Turner, A.D.; Hernández-Sandoval, F.E.; Okolodkov, Y.B.; Fernández-Herrera, L.J.; Bustillos-Guzmán, J.J. Paralytic Shellfish Toxins of *Pyrodinium bahamense* (Dinophyceae) in the Southeastern Gulf of Mexico. *Toxins* **2022**, *14*, 760. [CrossRef]
42. Vargo, G.A. A brief summary of the physiology and ecology of *Karenia brevis* Davis (*G. Hansen* and *Moestrup* comb. nov.) red tides on the West Florida Shelf and of hypotheses posed for their initiation, growth, maintenance, and termination. *Harmful Algae* **2009**, *8*, 573–584. [CrossRef]
43. Tampa Bay Water Atlas Tampa Bay Water Atlas. Available online: https://www.tampabay.wateratlas.usf.edu/ (accessed on 27 January 2023).
44. Paerl, H.W.; Rudek, J.; Mallin, M.A. Stimulation of phytoplankton production in coastal waters by natural rainfall inputs: Nutritional and trophic implications. *Mar. Biol.* **1990**, *107*, 247–254. [CrossRef]
45. Dixon, L.K.; Kirkpatrick, G.J. *Biological Effects of Atmospheric Deposition on Algal Assemblages*; Mote Marine Laboratory: Sarasota, FL, USA, 1999.
46. Pucher, M.; Wünsch, U.; Weigelhofer, G.; Murphy, K.; Hein, T.; Graeber, D. staRdom: Versatile Software for Analyzing Spectroscopic Data of Dissolved Organic Matter in R. *Water* **2019**, *11*, 2366. [CrossRef]
47. Weishaar, J.L.; Aiken, G.R.; Bergamaschi, B.A.; Fram, M.S.; Fujii, R.; Mopper, K. Evaluation of specific ultraviolet absorbance as an indicator of the chemical composition and reactivity of dissolved organic carbon. *Environ. Sci. Technol.* **2003**, *37*, 4702–4708. [CrossRef]
48. Ohno, T. Fluorescence inner-filtering correction for determining the humification index of dissolved organic matter. *Environ. Sci. Technol.* **2002**, *36*, 742–746. [CrossRef] [PubMed]
49. Zech, W.; Senesi, N.; Guggenberger, G.; Kaiser, K.; Lehmann, J.; Miano, T.M.; Miltner, A.; Schroth, G. Factors controlling humification and mineralization of soil organic matter in the tropics. *Geoderma* **1997**, *79*, 117–161. [CrossRef]
50. Murphy, K.R.; Stedmon, C.A.; Graeber, D.; Bro, R. Fluorescence spectroscopy and multi-way techniques. PARAFAC. *Anal. Methods* **2013**, *5*, 6557. [CrossRef]
51. Murphy, K.R.; Stedmon, C.A.; Wenig, P.; Bro, R. OpenFluor– an online spectral library of auto-fluorescence by organic compounds in the environment. *Anal. Methods* **2014**, *6*, 658–661. [CrossRef]
52. Coble, P.G. Marine Optical Biogeochemistry: The Chemistry of Ocean Color. *Chem. Rev.* **2007**, *107*, 402–418. [CrossRef]
53. Coble, P.G. Characterization of marine and terrestrial DOM in seawater using excitation-emission matrix spectroscopy. *Mar. Chem.* **1996**, *51*, 325–346. [CrossRef]
54. Coble, P.G.; Del Castillo, C.E.; Avril, B. Distribution and optical properties of CDOM in the Arabian Sea during the 1995 Southwest Monsoon. *Deep Sea Res. Part II Top. Stud. Oceanogr.* **1998**, *45*, 2195–2223. [CrossRef]
55. Coble, P.G.; Green, S.A.; Blough, N.V.; Gagosian, R.B. Characterization of dissolved organic matter in the Black Sea by fluorescence spectroscopy. *Nature* **1990**, *348*, 432–435. [CrossRef]

56. Guillard, R.R.; Stein, J.R. (Eds.) Division Rates. In *Handbook of Phycological Methods: Culture Methods and Growth Measurements*; Cambridge University Press: Cambridge, MA, USA, 1973; pp. 289–312.
57. Brooks, M.E.; Kristensen, K.; van Benthem, K.J.; Magnusson, A.; Berg, C.W.; Nielsen, A.; Skaug, H.J.; Mächler, M.; Bolker, B.M. glmmTMB Balances Speed and Flexibility Among Packages for Zero-inflated Generalized Linear Mixed Modeling. *R J.* **2017**, *9*, 378. [CrossRef]
58. Lüdecke, D.; Ben-Shachar, M.; Patil, I.; Waggoner, P.; Makowski, D. performance: An R Package for Assessment, Comparison and Testing of Statistical Models. *JOSS* **2021**, *6*, 3139. [CrossRef]
59. Hartig, F. DHARMa: Residual Diagnostics for Hierarchical (Multi-Level/Mixed) Regression Models. R Package Version 0.4.6. Available online: https://florianhartig.github.io/DHARMa/ (accessed on 7 November 2023).
60. Fox, J.; Weisberg, S. An R Companion to Applied Regression, Third Edition. Available online: https://www.john-fox.ca/Companion/index.html (accessed on 7 November 2023).
61. Lenth, R.; Bolker, B.; Buerkner, P.; Giné-Vázquez, I.; Herve, M.; Jung, M.; Love, J.; Miguez, F.; Riebl, H.; Singmann, H. R Package Emmeans: Estimated Marginal Means. Version: 1.8.9. Available online: https://cran.r-project.org/web/packages/emmeans/index.html (accessed on 7 November 2023).
62. Stedmon, C.A.; Markager, S. Resolving the variability in dissolved organic matter fluorescence in a temperate estuary and its catchment using PARAFAC analysis. *Limnol. Oceanogr.* **2005**, *50*, 686–697. [CrossRef]
63. Yang, L.; Chen, W.; Zhuang, W.-E.; Cheng, Q.; Li, W.; Wang, H.; Guo, W.; Chen, C.-T.A.; Liu, M. Characterization and bioavailability of rainwater dissolved organic matter at the southeast coast of China using absorption spectroscopy and fluorescence EEM-PARAFAC. *Estuar. Coast. Shelf Sci.* **2019**, *217*, 45–55. [CrossRef]
64. Painter, S.C.; Lapworth, D.J.; Woodward, E.M.S.; Kroeger, S.; Evans, C.D.; Mayor, D.J.; Sanders, R.J. Terrestrial dissolved organic matter distribution in the North Sea. *Sci. Total Environ.* **2018**, *630*, 630–647. [CrossRef]
65. Benner, R. Molecular indicators of the bioavailability of dissolved organic matter. In *Aquatic Ecosystems*; Elsevier: Amsterdam, The Netherlands, 2003; pp. 121–137. ISBN 9780122563713.
66. Walker, S.A.; Amon, R.M.W.; Stedmon, C.; Duan, S.; Louchouarn, P. The use of PARAFAC modeling to trace terrestrial dissolved organic matter and fingerprint water masses in coastal Canadian Arctic surface waters. *J. Geophys. Res.* **2009**, *114*, G4. [CrossRef]
67. Søndergaard, M.; Stedmon, C.A.; Borch, N.H. Fate of terrigenous dissolved organic matter (DOM) in estuaries: Aggregation and bioavailability. *Ophelia* **2003**, *57*, 161–176. [CrossRef]
68. Murphy, K.R.; Stedmon, C.A.; Waite, T.D.; Ruiz, G.M. Distinguishing between terrestrial and autochthonous organic matter sources in marine environments using fluorescence spectroscopy. *Mar. Chem.* **2008**, *108*, 40–58. [CrossRef]
69. Dall'Osto, M.; Vaqué, D.; Sotomayor-Garcia, A.; Cabrera-Brufau, M.; Estrada, M.; Buchaca, T.; Soler, M.; Nunes, S.; Zeppenfeld, S.; van Pinxteren, M.; et al. Sea Ice Microbiota in the Antarctic Peninsula Modulates Cloud-Relevant Sea Spray Aerosol Production. *Front. Mar. Sci.* **2022**, *9*, 827061. [CrossRef]
70. Osburn, C.L.; Handsel, L.T.; Mikan, M.P.; Paerl, H.W.; Montgomery, M.T. Fluorescence tracking of dissolved and particulate organic matter quality in a river-dominated estuary. *Environ. Sci. Technol.* **2012**, *46*, 8628–8636. [CrossRef] [PubMed]
71. Fellman, J.B.; Petrone, K.C.; Grierson, P.F. Source, biogeochemical cycling, and fluorescence characteristics of dissolved organic matter in an agro-urban estuary. *Limnol. Oceanogr.* **2011**, *56*, 243–256. [CrossRef]
72. Wu, H.; Xu, X.; Fu, P.; Cheng, W.; Fu, C. Responses of soil WEOM quantity and quality to freeze–thaw and litter manipulation with contrasting soil water content: A laboratory experiment. *Catena* **2021**, *198*, 105058. [CrossRef]
73. Castillo, C.R.; Sarmento, H.; Álvarez-Salgado, X.A.; Gasol, J.M.; Marraséa, C. Production of chromophoric dissolved organic matter by marine phytoplankton. *Limnol. Oceanogr.* **2010**, *55*, 446–454. [CrossRef]
74. Suksomjit, M.; Nagao, S.; Ichimi, K.; Yamada, T.; Tada, K. Variation of dissolved organic matter and fluorescence characteristics before, during and after phytoplankton bloom. *J. Oceanogr.* **2009**, *65*, 835–846. [CrossRef]
75. Romera-Castillo, C.; Sarmento, H.; Alvarez-Salgado, X.A.; Gasol, J.M.; Marrasé, C. Net production and consumption of fluorescent colored dissolved organic matter by natural bacterial assemblages growing on marine phytoplankton exudates. *Appl. Environ. Microbiol.* **2011**, *77*, 7490–7498. [CrossRef]
76. Muni-Morgan, A.; Lusk, M.G.; Heil, C.; Goeckner, A.H.; Chen, H.; McKenna, A.M.; Holland, P.S. Molecular characterization of dissolved organic matter in urban stormwater pond and municipal wastewater discharges transformed by the Florida red tide dinoflagellate *Karenia brevis*. *Sci. Total Environ.* **2023**, *904*, 166291. [CrossRef]
77. Zimberlin, M. Nutrient Limitation of Bioluminescent Dinoflagellates in Mangrove Lagoon, Salt River Bay, St. Croix USVI. Master's Thesis, University of South Carolina, Columbia, SC, USA, 2013.
78. Glibert, P.M.; Wilkerson, F.P.; Dugdale, R.C.; Raven, J.A.; Dupont, C.L.; Leavitt, P.R.; Parker, A.E.; Burkholder, J.M.; Kana, T.M. Pluses and minuses of ammonium and nitrate uptake and assimilation by phytoplankton and implications for productivity and community composition, with emphasis on nitrogen-enriched conditions. *Limnol. Oceanogr.* **2016**, *61*, 165–197. [CrossRef]
79. Bronk, D.A.; Glibert, P.M.; Ward, B.B. Nitrogen uptake, dissolved organic nitrogen release, and new production. *Science* **1994**, *265*, 1843–1846. [CrossRef]
80. Gomez, A.M.; Lopez, J.C. Bringing color to sugars: The chemical assembly of carbohydrates to BODIPY dyes. *Chem. Rec.* **2021**, *21*, 3112–3130. [CrossRef] [PubMed]
81. Myklestad, S.M. Release of extracellular products by phytoplankton with special emphasis on polysaccharides. *Sci. Total Environ.* **1995**, *165*, 155–164. [CrossRef]

82. Usman, A.; Khalid, S.; Usman, A.; Hussain, Z.; Wang, Y. Algal polysaccharides, novel application, and outlook. In *Algae Based Polymers, Blends, and Composites*; Elsevier: Amsterdam, The Netherlands, 2017; pp. 115–153, ISBN 9780128123607.
83. Chen, J.; LeBoeuf, E.J.; Dai, S.; Gu, B. Fluorescence spectroscopic studies of natural organic matter fractions. *Chemosphere* **2003**, *50*, 639–647. [CrossRef]
84. Zhang, Y.; Liu, X.; Wang, M.; Qin, B. Compositional differences of chromophoric dissolved organic matter derived from phytoplankton and macrophytes. *Org. Geochem.* **2013**, *55*, 26–37. [CrossRef]
85. Bronk, D.A.; Killberg-Thoreson, L.; Sipler, R.E.; Mulholland, M.R.; Roberts, Q.N.; Bernhardt, P.W.; Garrett, M.; O'Neil, J.M.; Heil, C.A. Nitrogen uptake and regeneration (ammonium regeneration, nitrification and photoproduction) in waters of the West Florida Shelf prone to blooms of *Karenia brevis*. *Harmful Algae* **2014**, *38*, 50–62. [CrossRef]
86. Azam, F.; Fenchel, T.; Field, J.G.; Gray, J.S.; Meyer-Reil, L.A.; Thingstad, F. The Ecological Role of Water-Column Microbes in the Sea. *Mar. Ecol. Prog. Ser.* **1983**, *10*, 257–263. [CrossRef]
87. Bronk, D.A.; See, J.H.; Bradley, P.; Killberg, L. DON as a source of bioavailable nitrogen for phytoplankton. *Biogeosciences* **2007**, *4*, 283–296. [CrossRef]
88. Heil, C.A.; Steidinger, K.A. Monitoring, management, and mitigation of *Karenia* blooms in the eastern Gulf of Mexico. *Harmful Algae* **2009**, *8*, 611–617. [CrossRef]
89. Turley, B.D.; Karnauskas, M.; Campbell, M.D.; Hanisko, D.S.; Kelble, C.R. Relationships between blooms of *Karenia brevis* and hypoxia across the West Florida Shelf. *Harmful Algae* **2022**, *114*, 102223. [CrossRef]
90. Stumpf, R.P.; Li, Y.; Kirkpatrick, B.; Litaker, R.W.; Hubbard, K.A.; Currier, R.D.; Harrison, K.K.; Tomlinson, M.C. Quantifying *Karenia brevis* bloom severity and respiratory irritation impact along the shoreline of Southwest Florida. *PLoS ONE* **2022**, *17*, e0260755. [CrossRef]
91. Landsberg, J.H.; Hall, S.; Johannessen, J.N.; White, K.D.; Conrad, S.M.; Abbott, J.P.; Flewelling, L.J.; Richardson, R.W.; Dickey, R.W.; Jester, E.L.E.; et al. Saxitoxin puffer fish poisoning in the United States, with the first report of *Pyrodinium bahamense* as the putative toxin source. *Environ. Health Perspect.* **2006**, *114*, 1502–1507. [CrossRef] [PubMed]
92. Corcoran, A.A.; Wolny, J.; Leone, E.; Ivey, J.; Murasko, S. Drivers of phytoplankton dynamics in old Tampa Bay, FL (USA), a subestuary lagging in ecosystem recovery. *Estuar. Coast. Shelf Sci.* **2017**, *185*, 130–140. [CrossRef]
93. Greening, H.; Janicki, A.; Sherwood, E.T.; Pribble, R.; Johansson, J.O.R. Ecosystem responses to long-term nutrient management in an urban estuary: Tampa Bay, Florida, USA. *Estuar. Coast. Shelf Sci.* **2014**, *151*, A1–A16. [CrossRef]